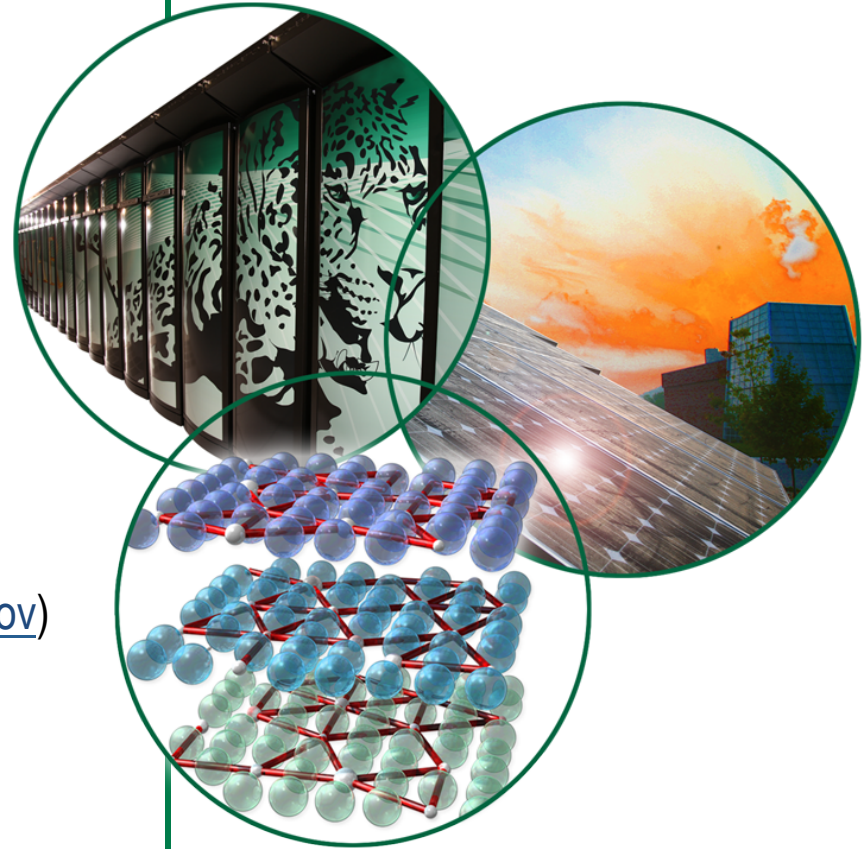


Introduction to Neutron Imaging

Neutron Imaging Team

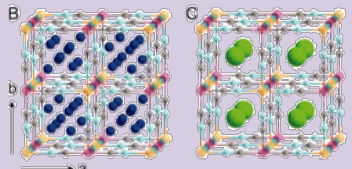
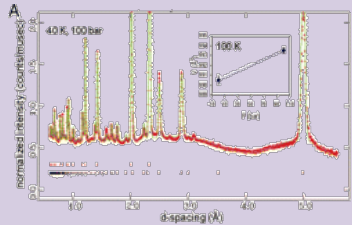
Lou Santodonato, Scientific Associate
Jean Bilheux, Data Reduction and Analysis
Barton Bailey, Engineer
Hassina Bilheux, Instrument Scientist (bilheuxhn@ornl.gov)

NX School
June 25, 2014

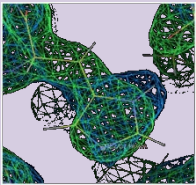


Neutrons Measure Structure

Neutron Diffraction

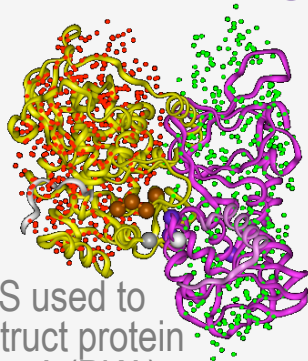


Neutron diffraction of D_2 sorption in $Cu_3[Co(CN)_6]_2$

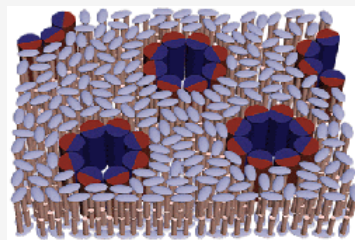


Nuclear and electronic density in enzymes

Neutron Scattering

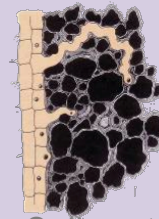


SANS used to construct protein kinase A (PKA)

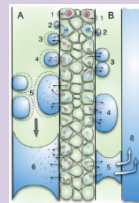


Characterization of biological membranes, colloids, porosity, etc.

Neutron Microscopy



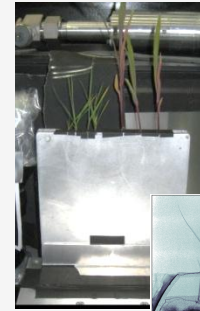
Soil-root interface (rhizosphere)



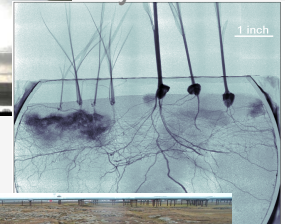
Computed tomography

In Vivo Study of Embolism Formation

Neutron Imaging



Fluid interactions in plant-groundwater systems



Ice/water segregation in permafrost structures

Inferred structure (indirect)

Direct structure

10^{-11}

10^{-9}

10^{-7}

10^{-5}

10^{-3}

Dimension (meters)

0.1 Å

1.0 nm

0.1 μm

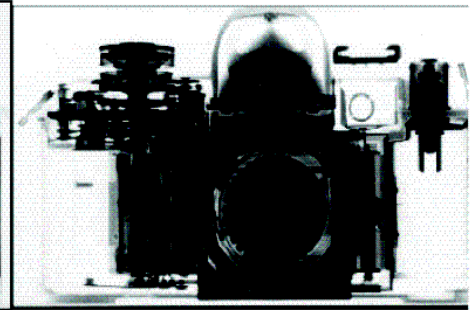
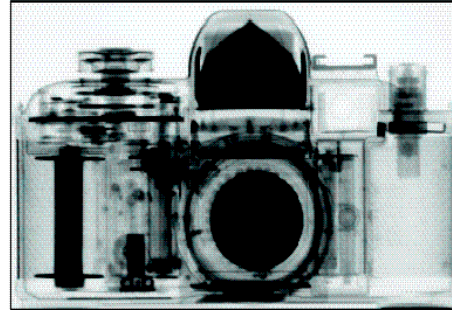
10.0 μm

1 mm

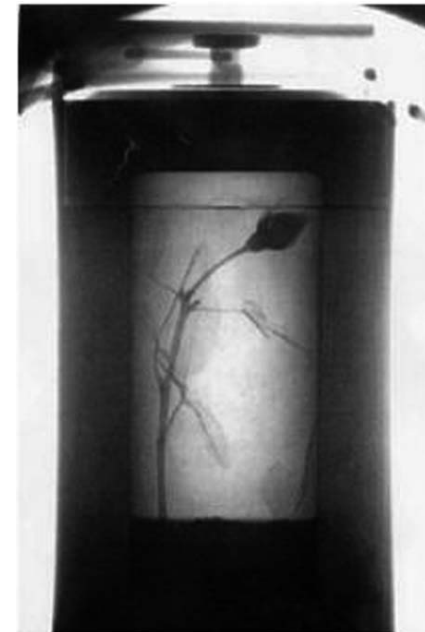
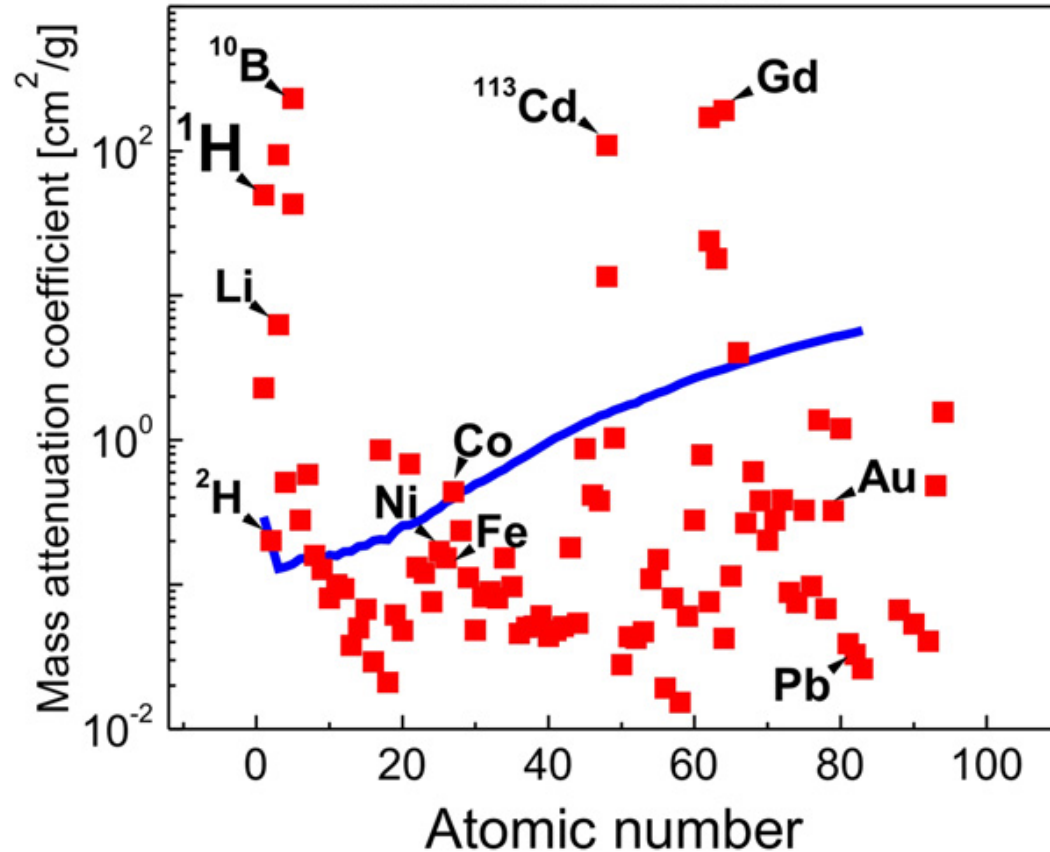
Neutron sensitivity

Neutron Radiograph of camera

X-ray Radiograph of camera



— X-rays (100 keV)
 ■ Thermal neutrons



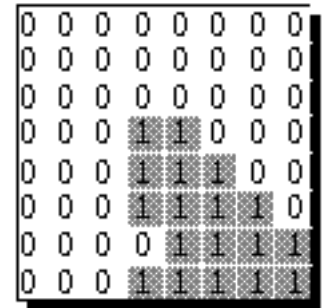
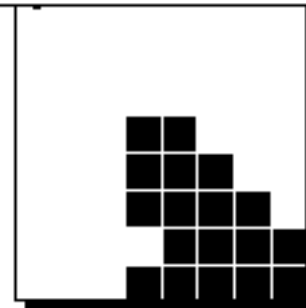
Neutron Radiograph of Rose in Lead Flask

[M. Strobl et al., *J. Phys. D: Appl. Phys.* **42** (2009) 243001]

Courtesy of E. Lehmann, PSI

What is imaging?

- **Imaging** is the visual representation of an object: photography, cinematography, medical imaging, X-ray imaging, thermal imaging, molecular imaging, neutron imaging, etc.



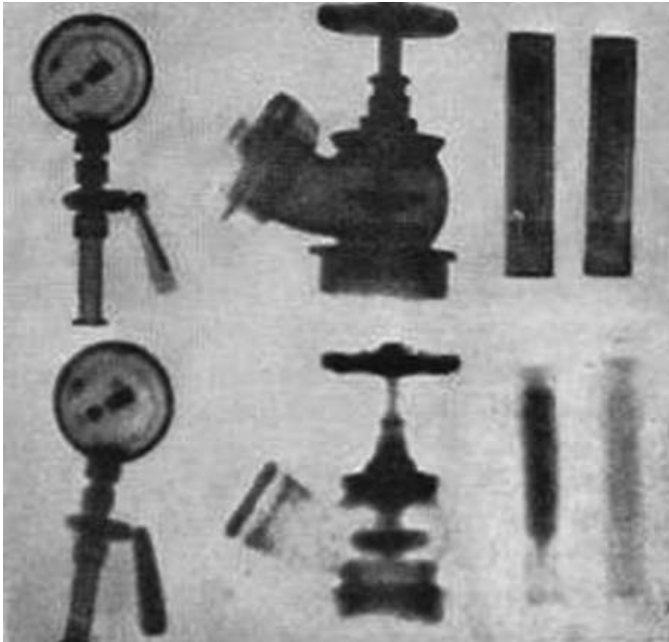
- **Digital Imaging** is a field of computer science covering images that can be stored on a computer as *bit-mapped images*

Image Modalities and Imaging Science & Technology throughout Nobel Prize history

- 1901: Roentgen, FIRST Nobel Prize in Physics, **Discovery of X-rays**
- 1932: Chadwick, Nobel Prize in Physics **Discovery of Neutrons**
- 1979: Cormack and Hounsfield, Nobel Prize in Medicine, **Computed Tomography (CT)**
- 1986: Ruska, Binnig, Rohrer, Nobel Prize in Physics, **Electron Microscopy**
- 2003: Lauterbur and Mansfield, Nobel Prize in Medicine, **Magnetic Resonance Imaging (MRI)**
- 2009: Boyle and Smith, Nobel Prize in Physics, **Imaging semi-conductor circuit, the CCD* sensor**

Early neutron imaging measurements

- Neutron Imaging started in the mid 1930's but only during the past 30 years has it come to the forefront of non-destructive testing



Discovery of neutron in 1932 by Chadwick

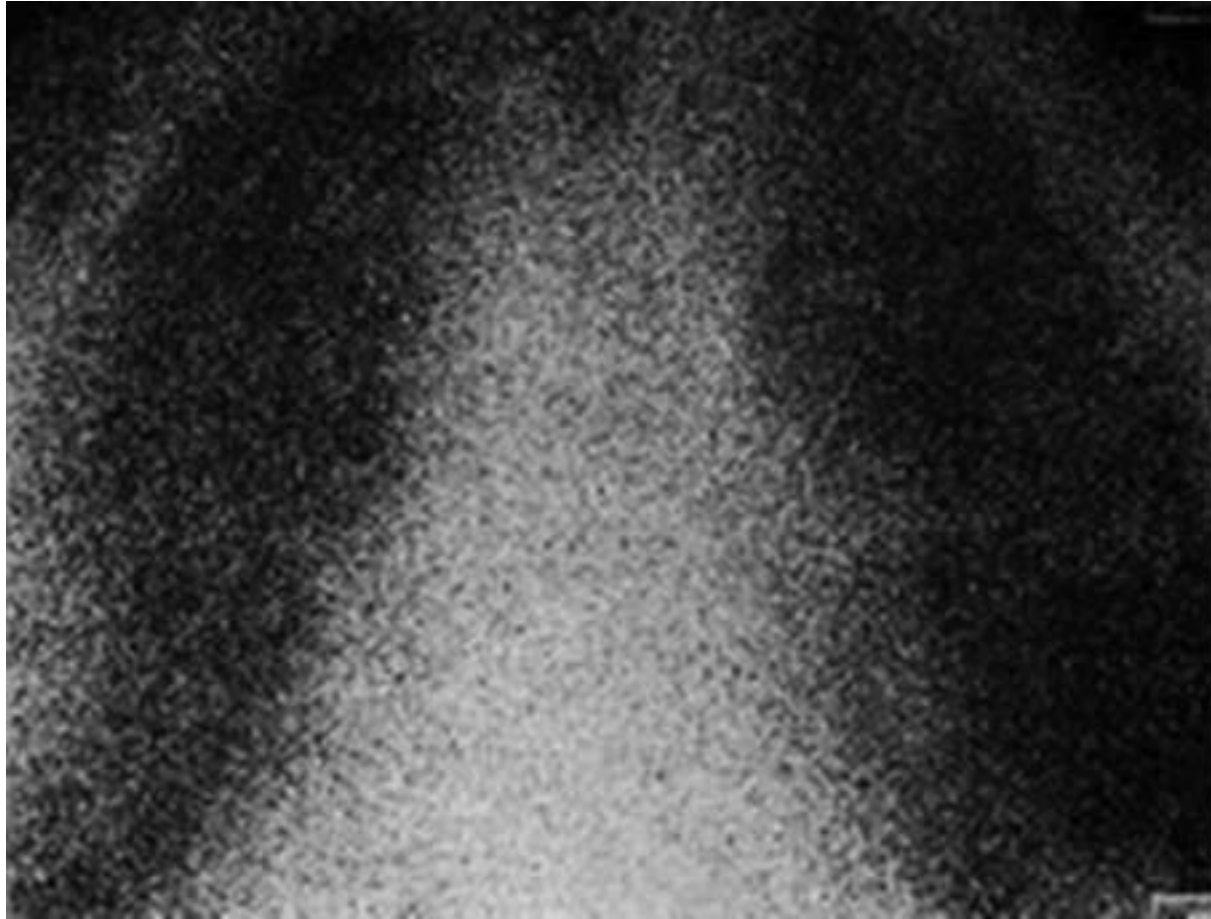
First neutron radiograph in 1935

Left to right: Pressure gauge with metal backplate; fire hydrant and test tubes filled with H₂O and D₂O imaged with gamma-rays (top) and neutrons (bottom)

[Kallman and Kuhn, Research 1, 254 (1947)]

- Dedicated world class imaging user facilities such as NIST, PSI, HZB, FRM-II, J-PARC and at many worldwide universities
- World conferences and workshops being held regularly
- Growing worldwide user community

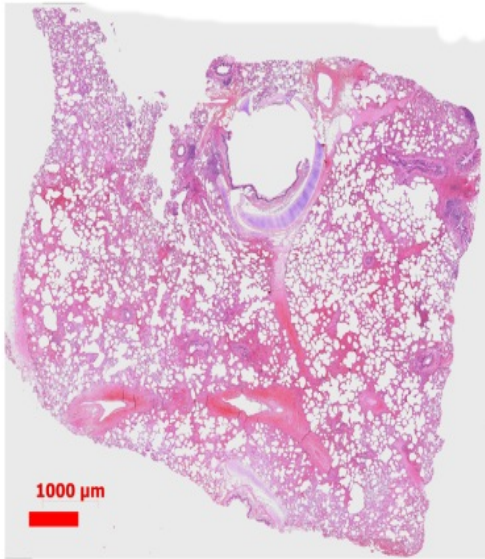
Multiple scattering and low detector spatial resolution



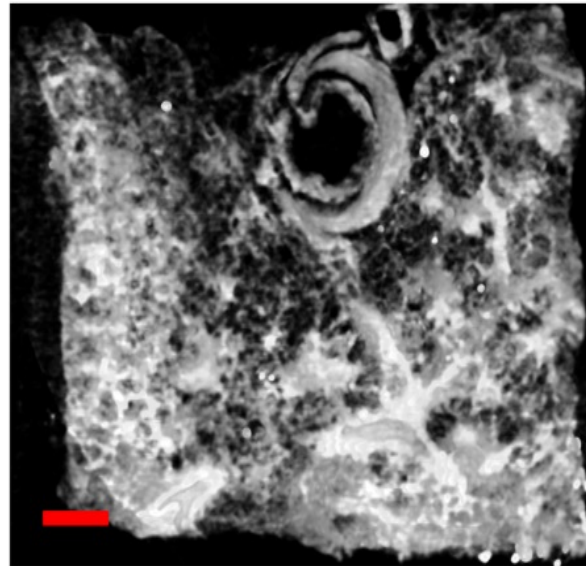
[J. Anderson et al., Br. J. Radiol. 37, 957 (1964)]

Today: Comparison microscopy/microCT and neutron radiography

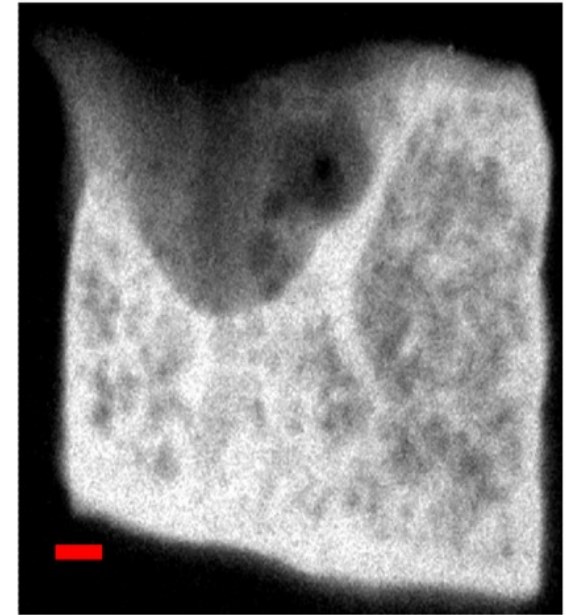
Microscope



microCT



Neutron

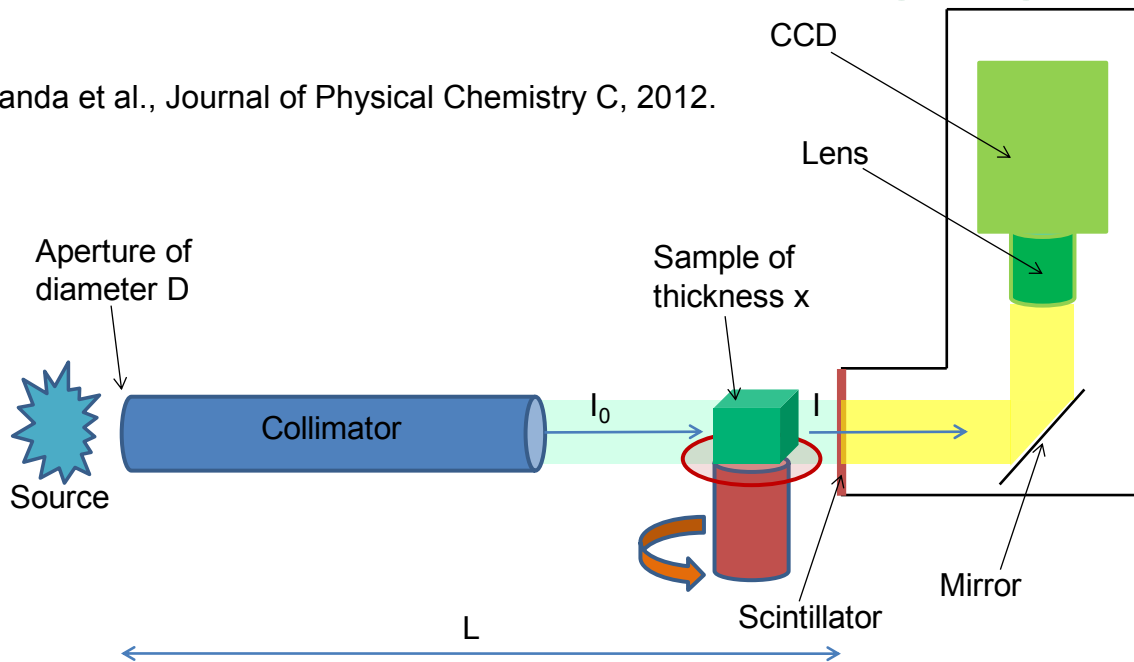


- 92% of the pixel intensities agreement between histological and neutron

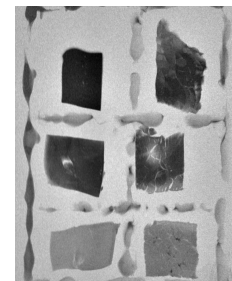
Watkin, K. et al., Neutron Imaging and Applications, Springer, 2009.

Basics of Neutron imaging

Nanda et al., Journal of Physical Chemistry C, 2012.



Photograph Neutron Radiograph



Beam attenuation caused by a **homogeneous uniformly** thick sample composed of a **single isotope** is given by

$$I(\lambda) = I_0(\lambda)e^{-\mu(\lambda)x}$$

$$\mu(\lambda) = \sigma_t(\lambda) \frac{\rho N_A}{M}$$

$\sigma_t(\lambda)$ = scattering and absorption

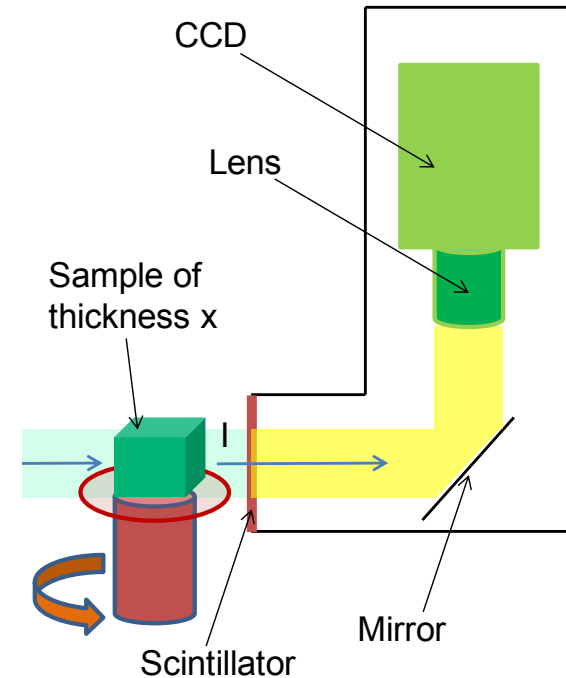
μ is the attenuation coefficient and Δx is the thickness of the sample

$\sigma_t(\lambda)$ is the material's total cross section for neutrons, ρ is its density, N_A is Avogadro's number, and M is the molar mass.

Detection of “imaging” neutrons

- Scintillator-based techniques such as ${}^6\text{Li}(n,\alpha) {}^3\text{H}$
 - Good signal-to-noise (SNR) ratio
 - Large Field Of View (FOV) and 0.01 to hundreds of seconds images
 - BUT spatial resolution limited by the dissipation of particles
 - Can take a lot of neutron flux!

1,1	1,2	1,3	1, ny
2,1	2,2	2,3	2, ny
3,1	3,2	3, ny
..., nx
nx, 1	nx, 2	nx, 3	nx, ny

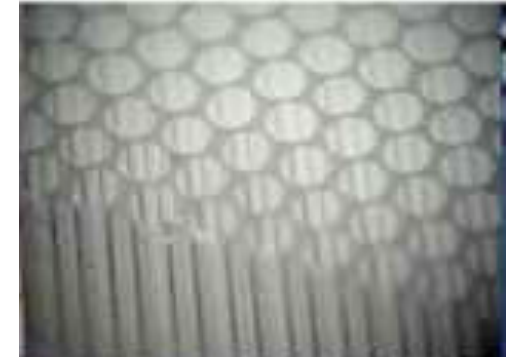


Each pixel is coded using n-bit.
16-bit = pixel value is between 0 and 65535

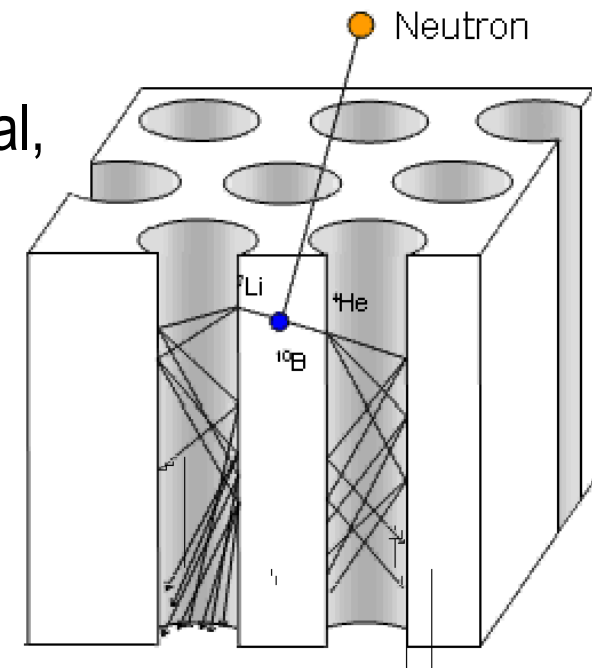
Detection of “imaging” neutrons (cont’d)

- Pixelated detectors

- Micro-Channel Plate (MCP)
- In the direct path of the beam
- Limited FOV for high spatial resolution MCPs
 - 1.4 cm x 1.4 cm at ~ 15 microns
- Encodes events at x, y position and time of arrival, at high temporal resolution ~ 1 MHz
- Detection efficiency has improved for both cold (~70%) and thermal (~50%) energy range
- Absence of readout noise
- Not as gamma sensitive
- Becoming commercial
- BUT: works in relatively low-signal beam!



Courtesy of Prof. A. Tremsin, UC-Berkeley

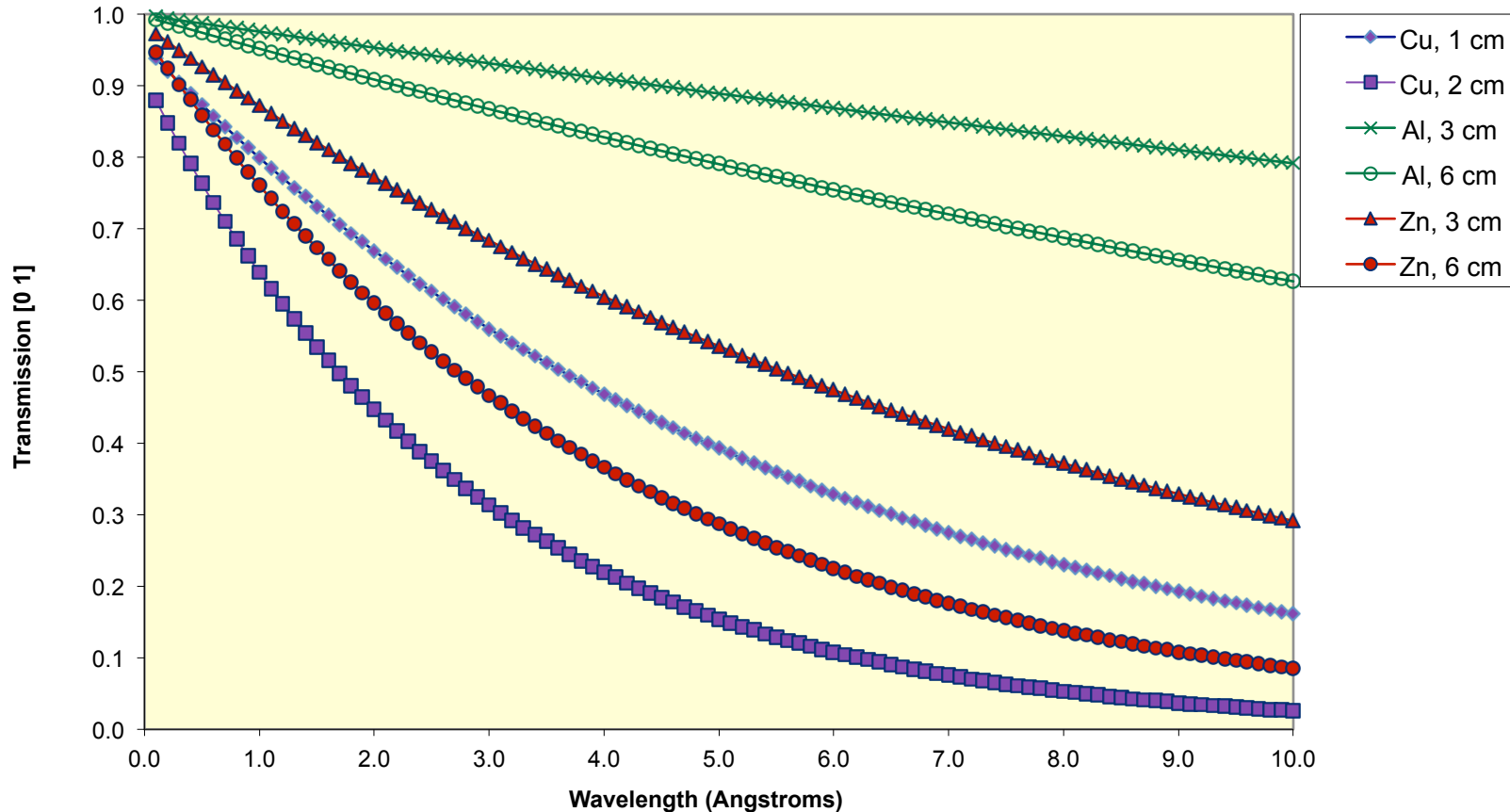


<http://www.novascientific.com/neutron.html>

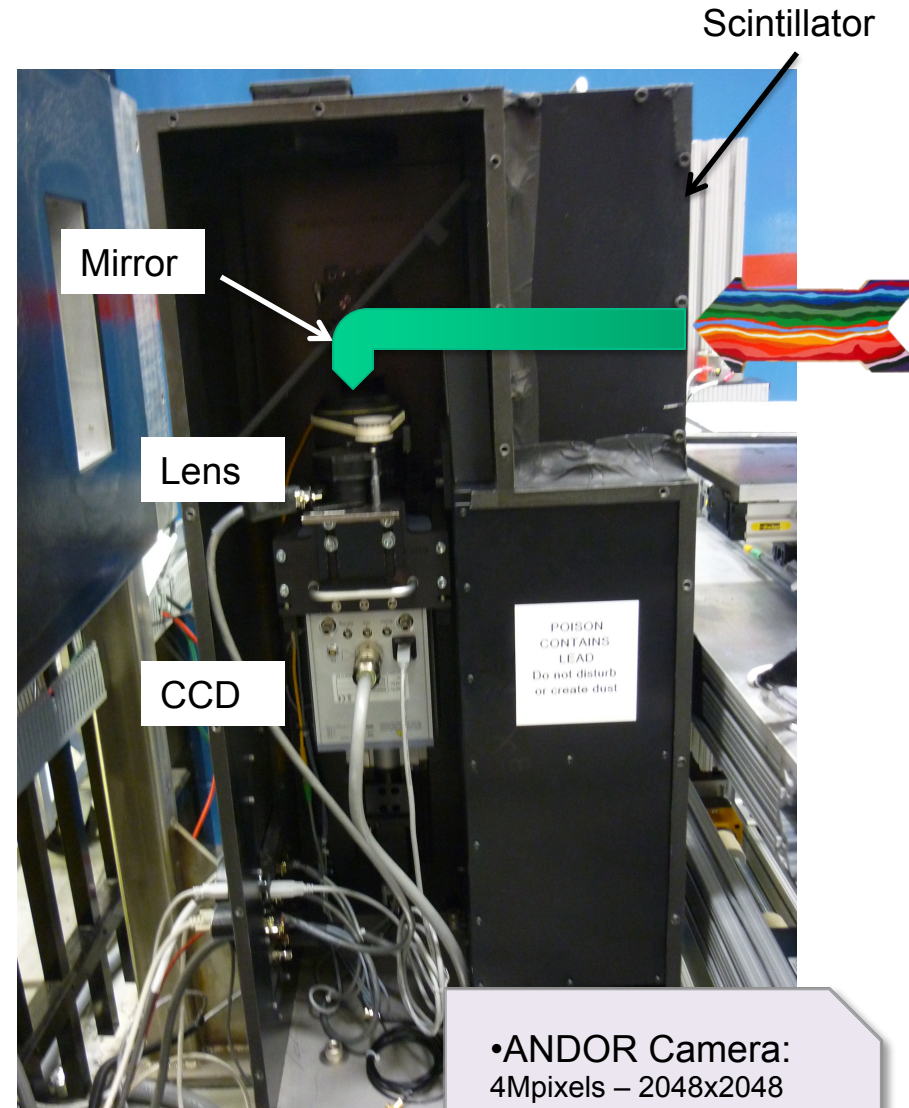
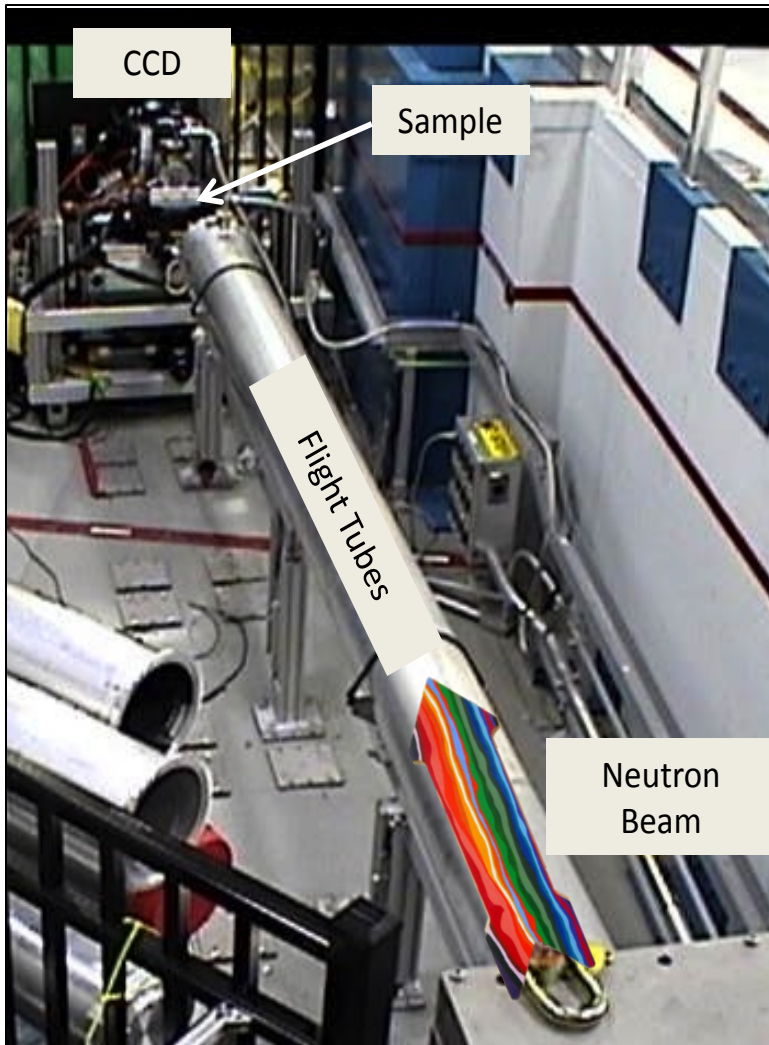
Example: Cu, Zn and Al

Compound	Abs. Coeff. [\AA^{-2}]	Inc. Coeff. [\AA^{-1}]
Cu (100%)	1.78E-09	4.65E-10
Al (100%)	7.75E-11	4.94E-12
Zn (100%)	4.06E-10	5.06E-11

Neutron Transmission through Metals

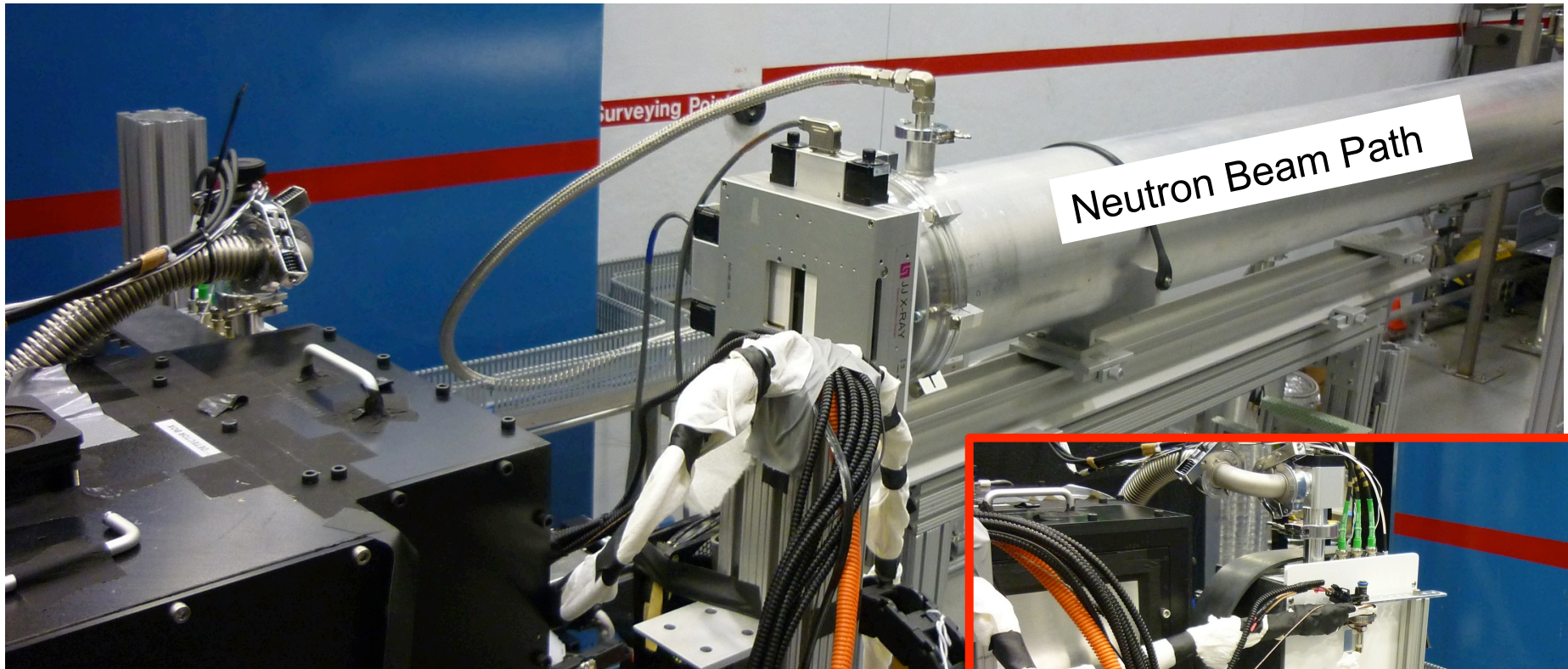


CG-1D Neutron Imaging Facility



- ANDOR Camera:
4Mpixels – 2048x2048
- Field of view:
7x7cm²
- Quantum Efficiency:
95%

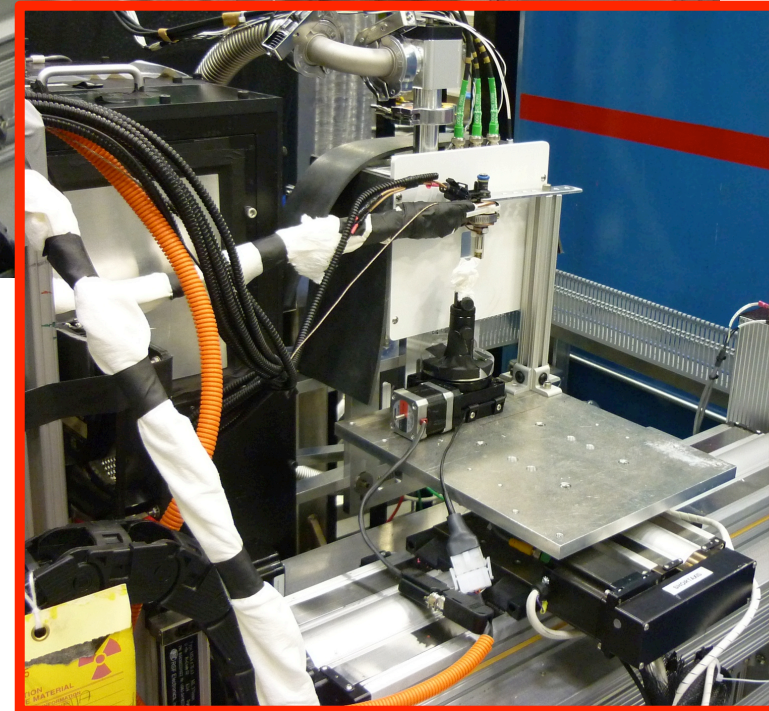
HFIR Neutron Imaging Facility (CG-1D)



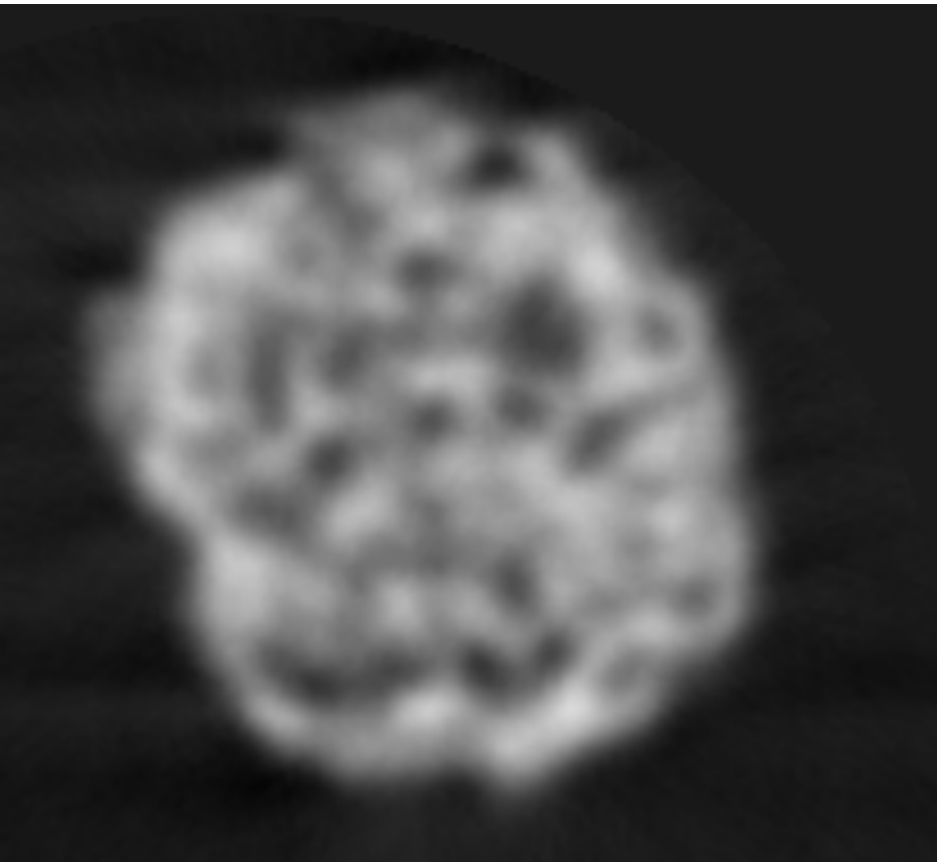
Detector capability/spatial resolution:
ANDOR® CCD Detector ~ 80 microns

MCP(*) ~ 25-50 microns (and ~ 15 microns in
centroiding mode)

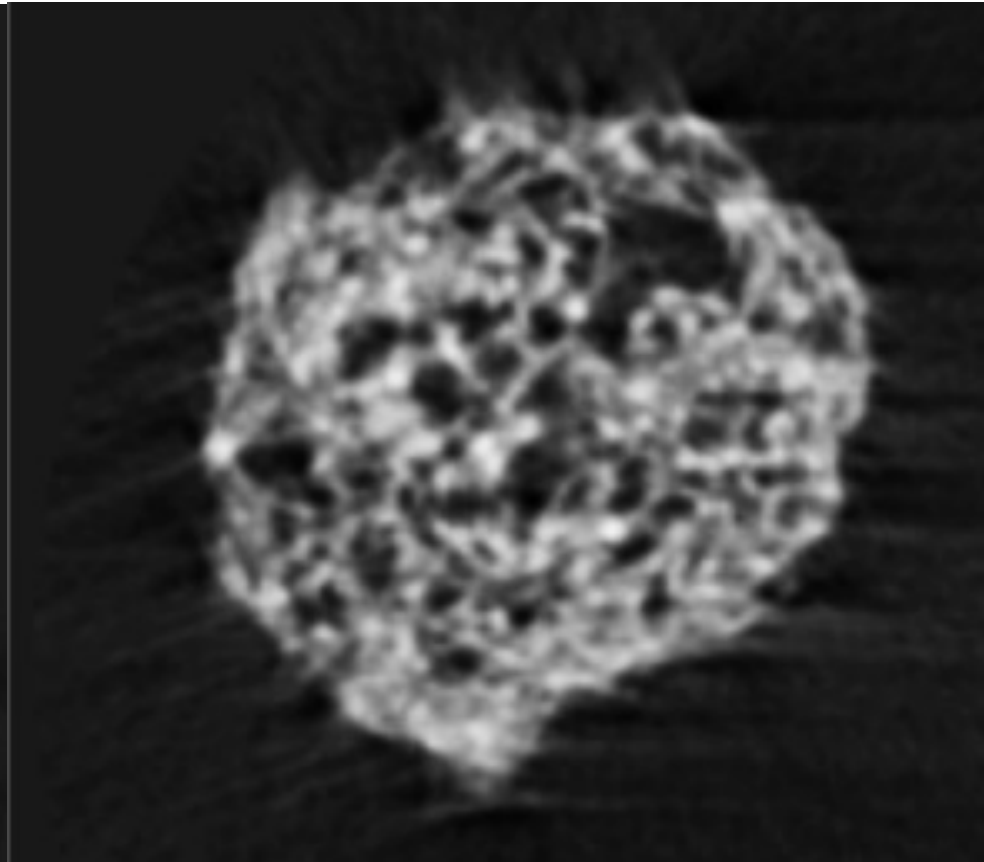
(*) In Collaboration with Prof. Anton
Tremis, UC-Berkeley



CCD and MCP spatial resolution comparison with the same cereal sample



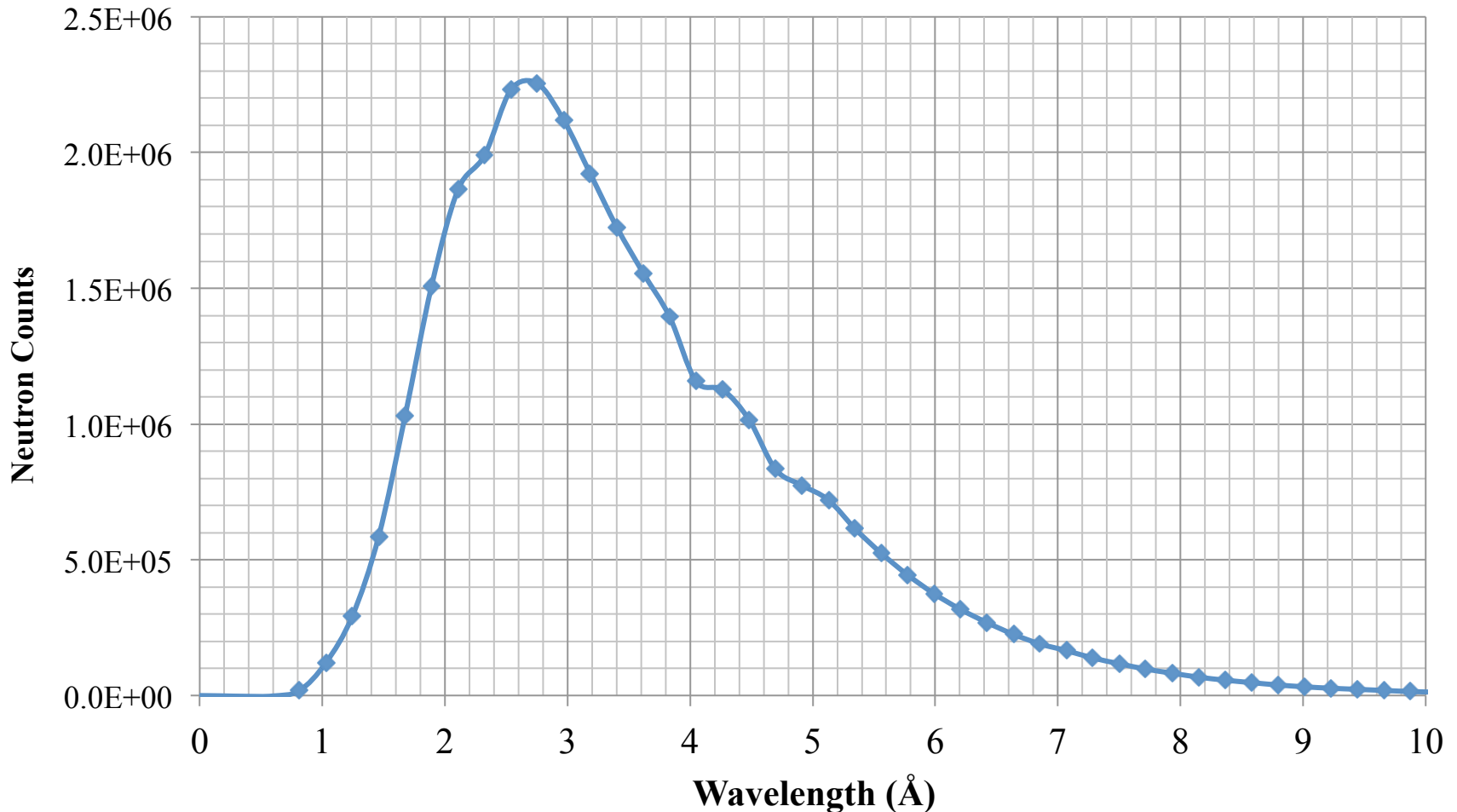
CCD CT Scan: 12 hrs



MCP CT scan: 4 hrs

Courtesy of Dr. Camille Loupiac (camille.loupiac@agrosupdijon.fr),
AgropSup-Dijon and CEA Saclay, France

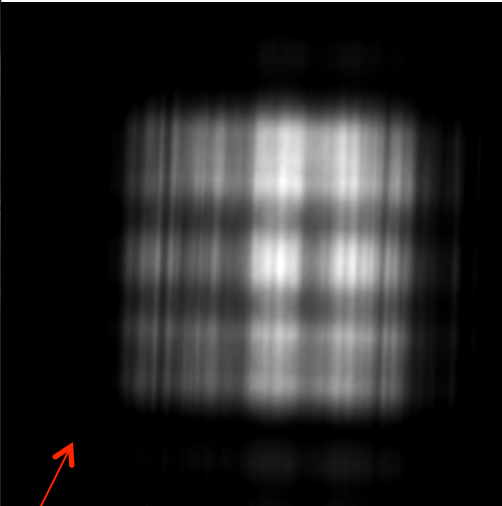
CG-1D polychromatic beam



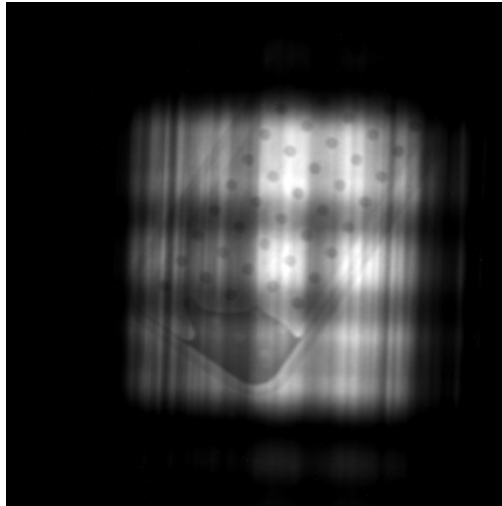
CG-1D spectrum measured with the MCP detector at a flight path distance of approximately 5.5 m, with the chopper running at a frequency 40 Hz and an 5 mm aperture. *[Bilheux et al., ITMNR-7, Canada, June 2012]*

Use of Diffusers

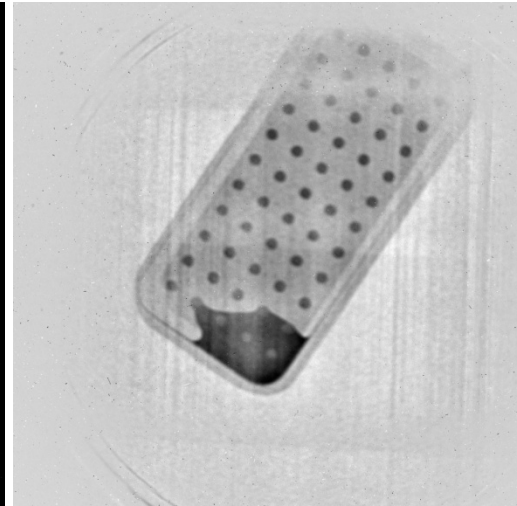
- 1 cm thick Graphite Powder (4 to 10 microns)



Open Beam



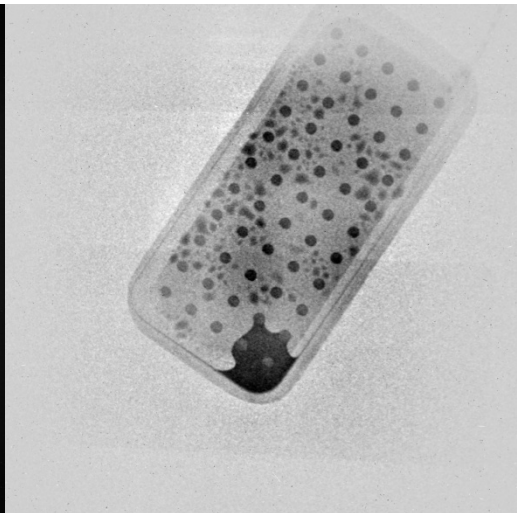
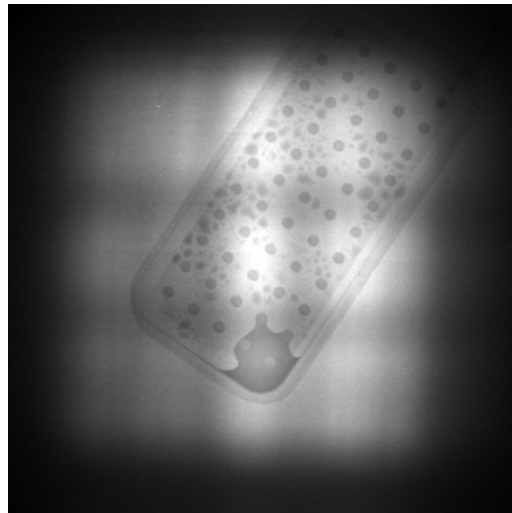
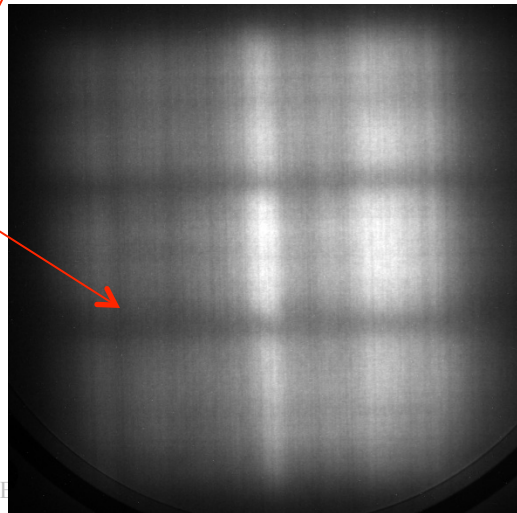
Heat Pipe Sample



Reduced Image

Without diffuser

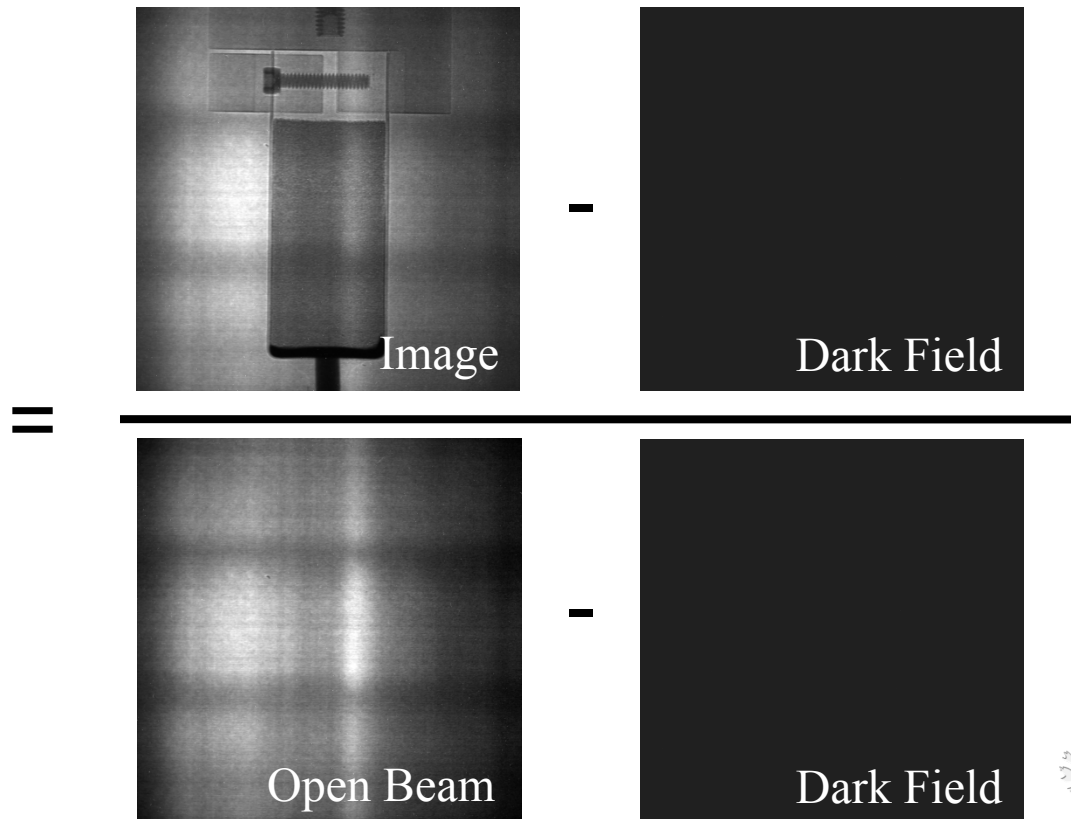
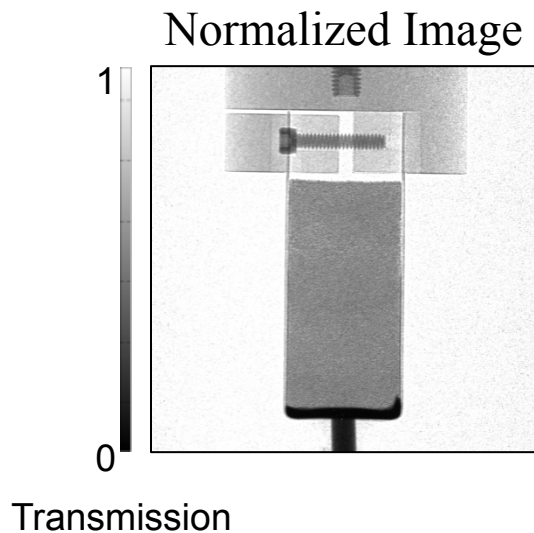
With diffuser



Data Normalization for Imaging

- 2D – Radiography
 - Normalization

$$I_N(i, j) = \frac{I(i, j) - DF(i, j)}{OB(i, j) - DF(i, j)}$$



Computed/Computerized Tomography (CT)

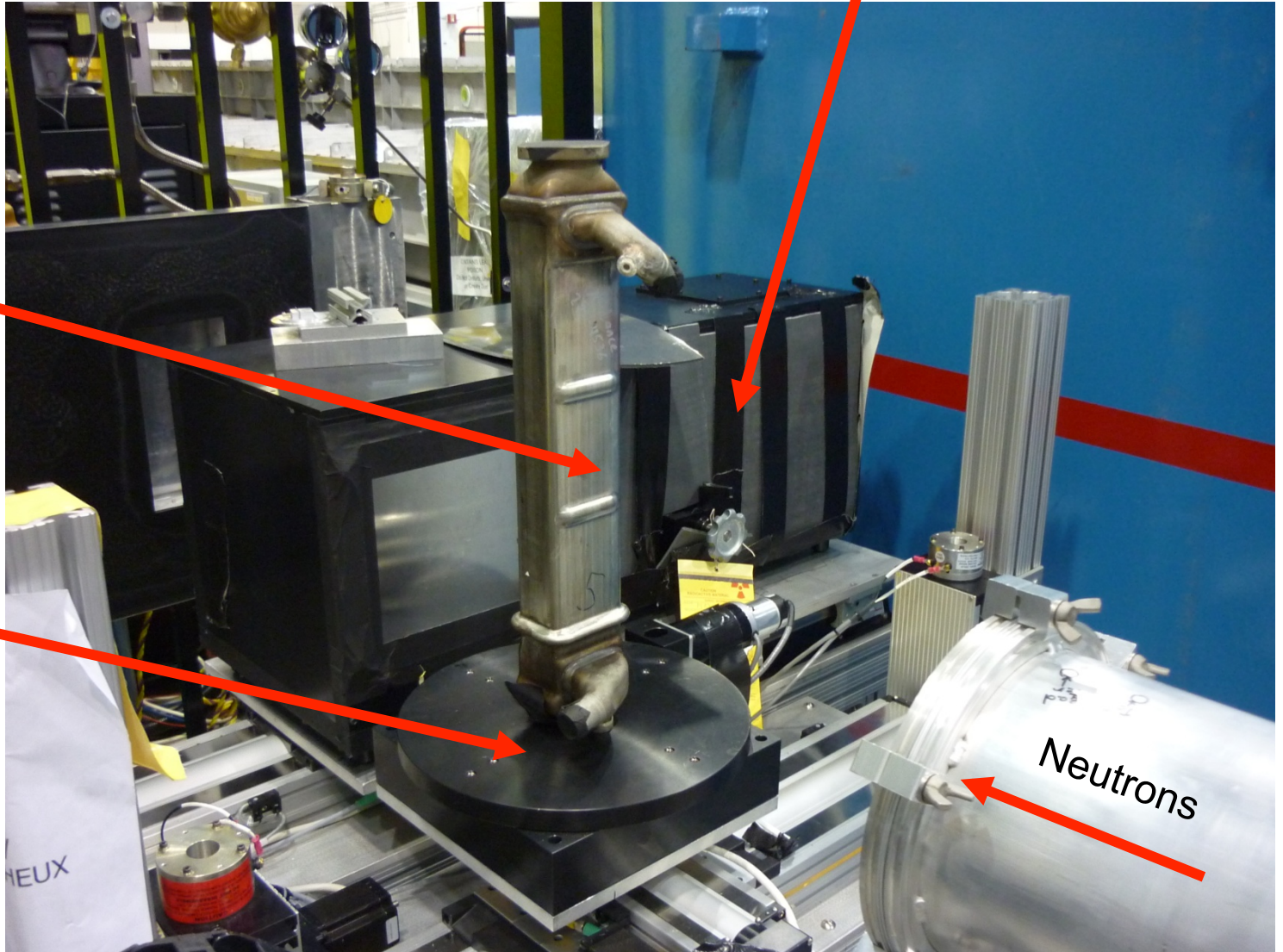
- **Several techniques:**
 - **Filtered Back Projection**
 - Radon transform
 - Works well with high signal to noise ratio measurements
 - Easy-to-use commercial, semi-automated software available
 - Quick
 - **Iterative Reconstruction**
 - Direct approach
 - Less artifacts
 - Can reconstruct incomplete data
 - High computation time

Sample stage for nCT

CCD Detector

EGR
Cooler

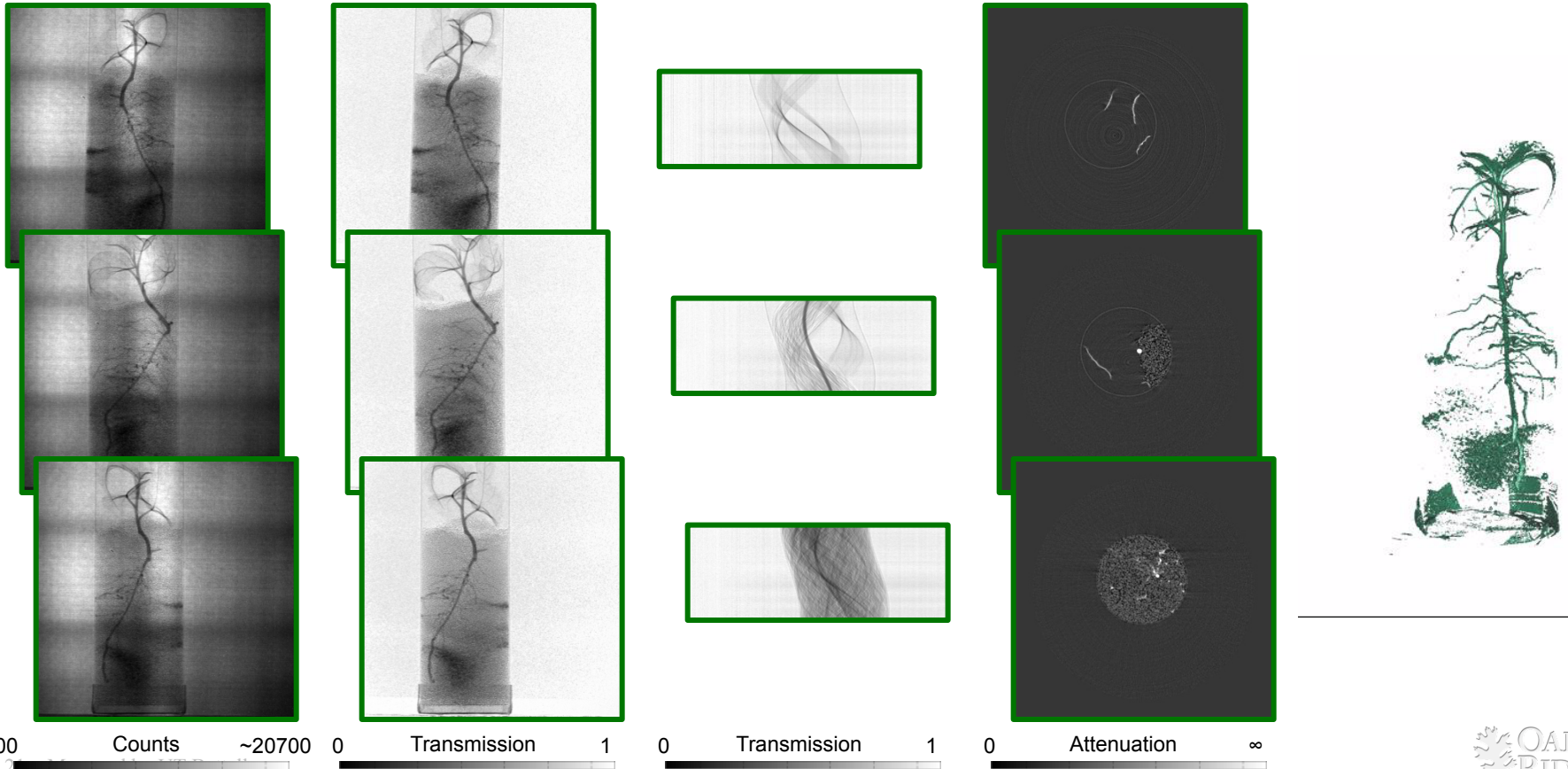
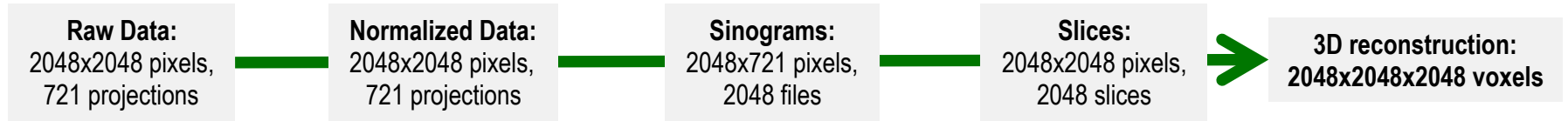
Rotation/
Translation
Stage



Neutrons

Computed/Computerized Tomography (FBP)

– Filtered back projection method



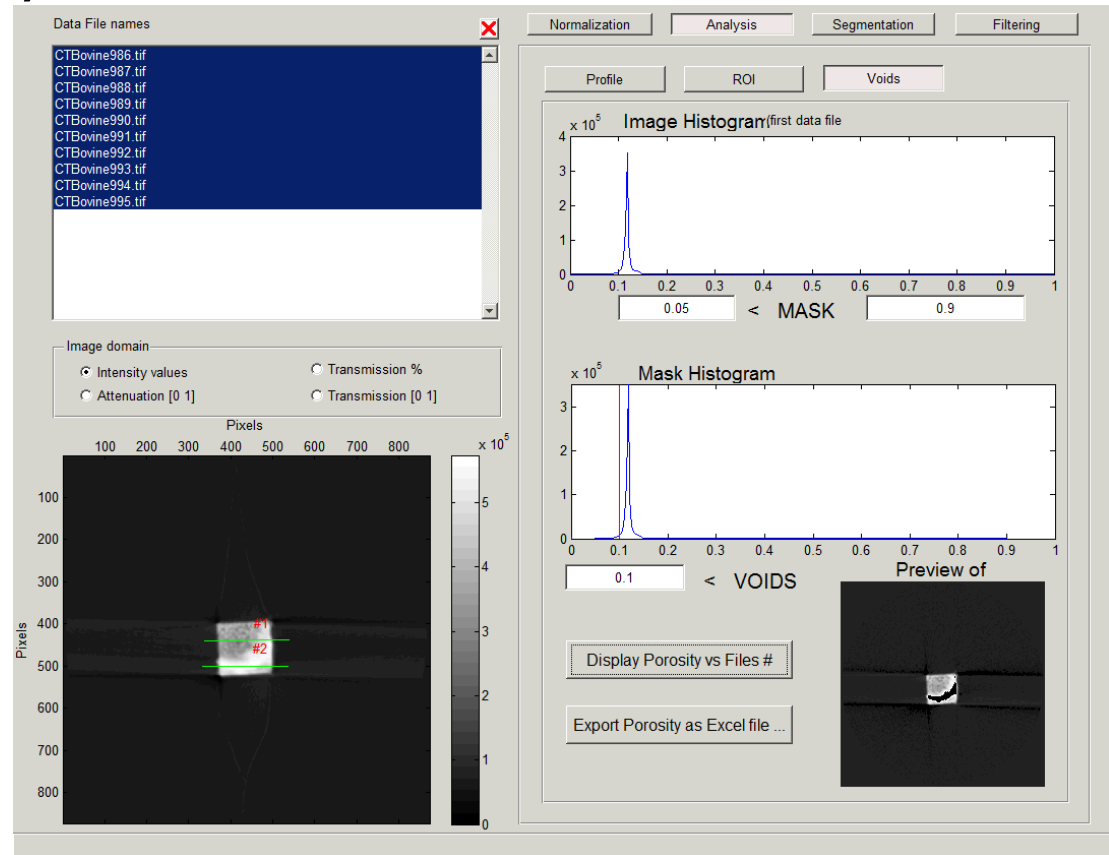
Data reduction and analysis software customized for scientific community

- Performed using software, (Matlab-based) and/or VGStudio (commercial software)

We develop tools users can utilize to perform their analysis:

-Software engineer interacts with users on a case by case basis
- Calibrated data sets used to test new module

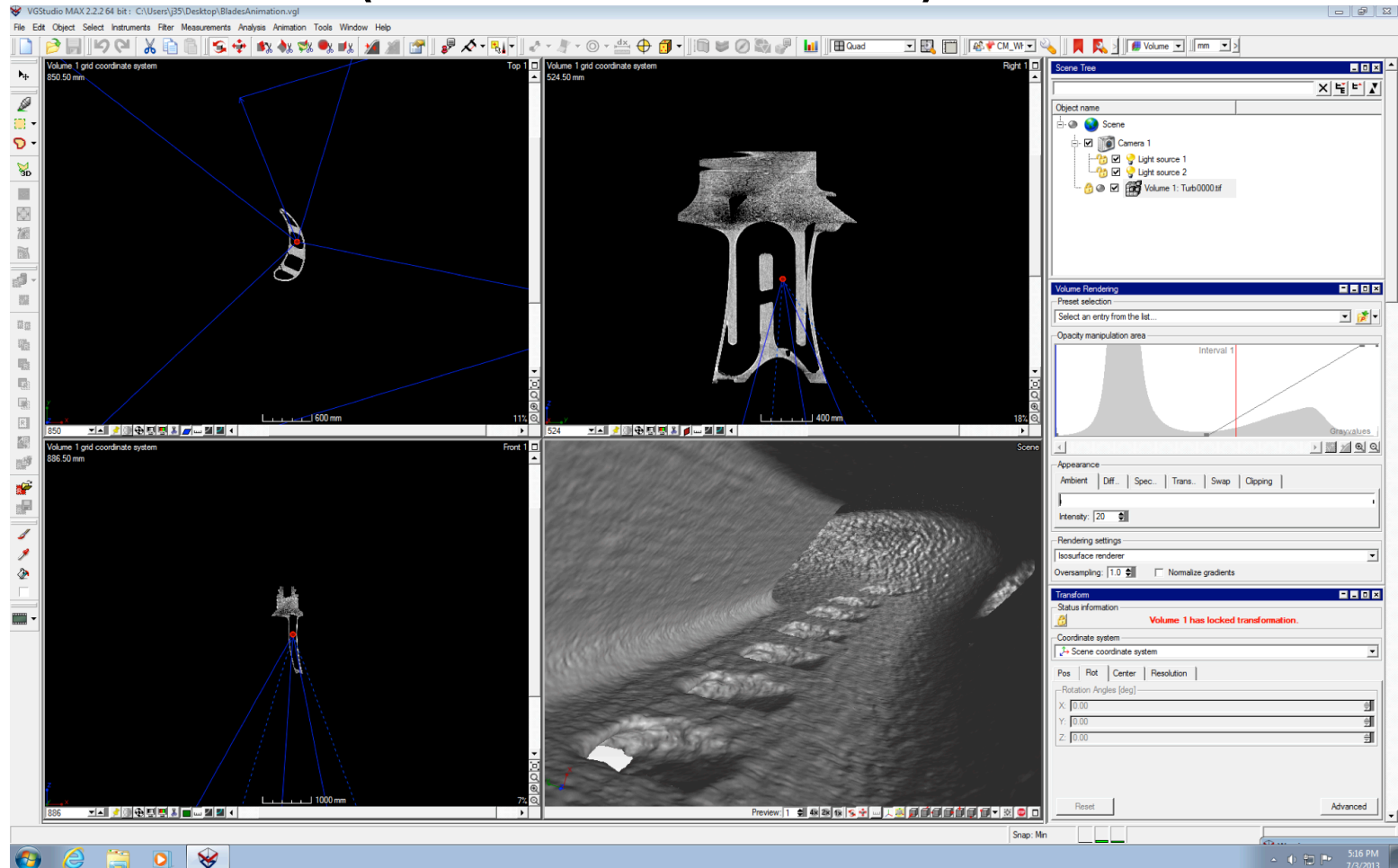
- ✓ Normalization
- ✓ Profiles
- ✓ ROIs
- ✓ Voids and Porosity
- ✓ Segmentation
- ✓ Filters (ISS)



We continue to use VisIt for large data sets (create VTK file using MatLab code).

Data analysis

- Performed using iMARS (Neutron Sciences software) and/or **VGStudio** (commercial software)



Conventional Neutron Imaging Techniques at steady-state sources

- Radiography (available at CG-1D)
- Tomography (available at CG-1D)
- Phase Contrast Imaging
- Polarized Neutron Imaging
- Stroboscopic Imaging
- Imaging of processes that happen fast
- Energy selective techniques possible with double-monochromator configuration

Neutron Imaging Techniques at pulsed sources

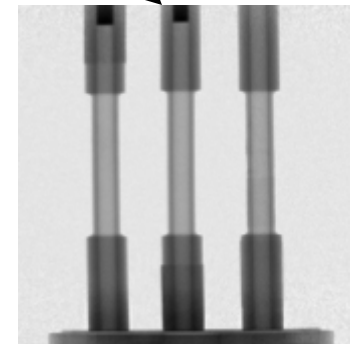
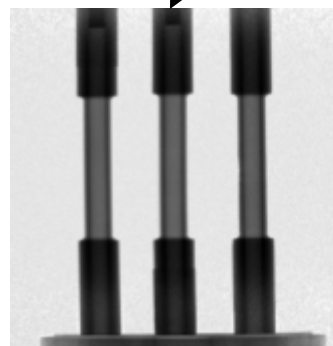
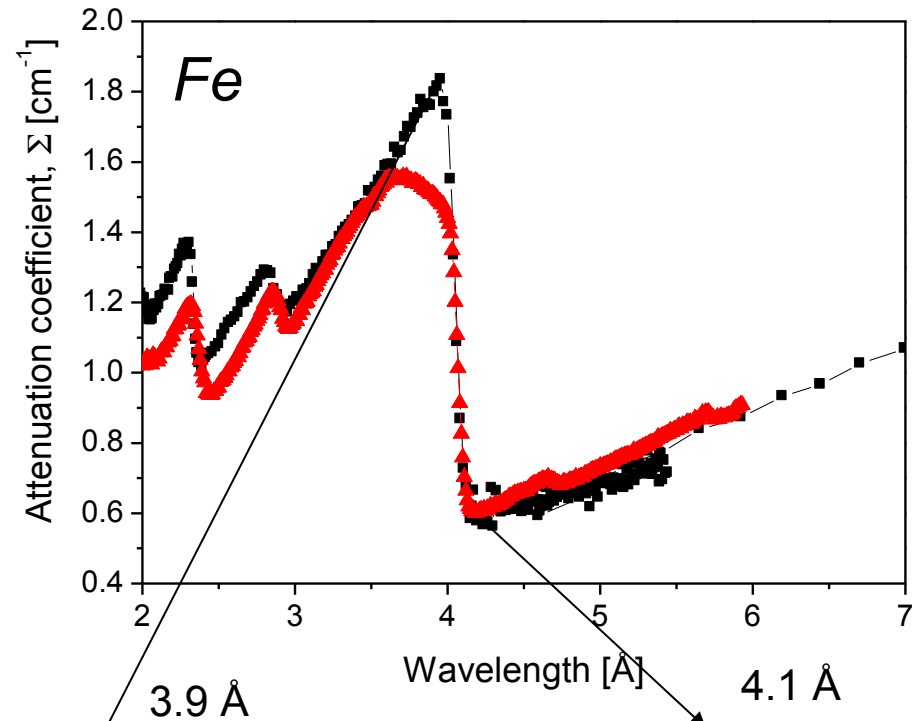
- **Energy-selective (or Time-of-Flight) imaging**
 - Contrast enhancement
 - Bragg edge
- **Stroboscopic imaging**
 - SNS has a natural clock
- **Neutron Imaging at energies not accessible at reactor facilities**
 - Mainly bio-medical applications

Neutron imaging techniques

- Radiography
- Computed tomography
- Bragg edge imaging
- Neutron phase imaging
- Stroboscopic imaging
- Neutron Stimulated Computed Emission Tomography or NSECT
- Polarized imaging
- Dark field imaging
- Energy resonance imaging

Bragg Edge Imaging

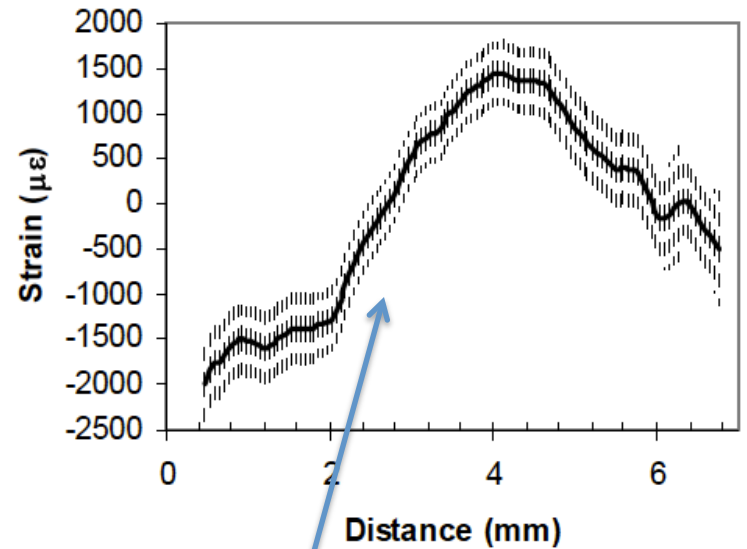
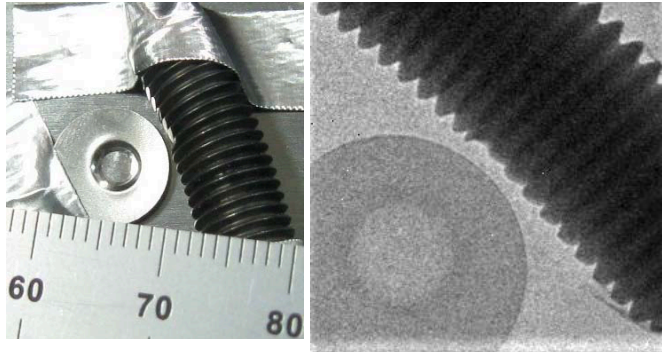
- **At reactors:**
 - monochromatic beams
 - Scintillator-based detection adequate
- **At spallation sources:**
 - Time-stamping of neutrons
 - Pixelated detectors such as MCPs required for time measurements



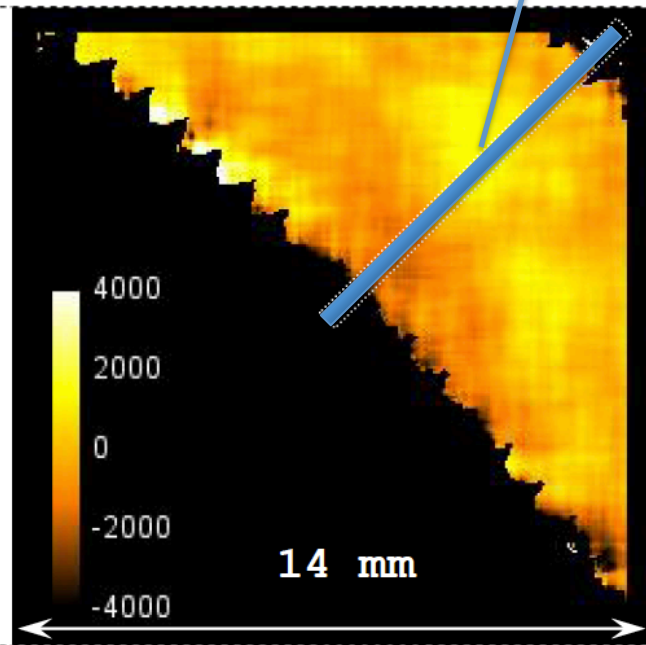
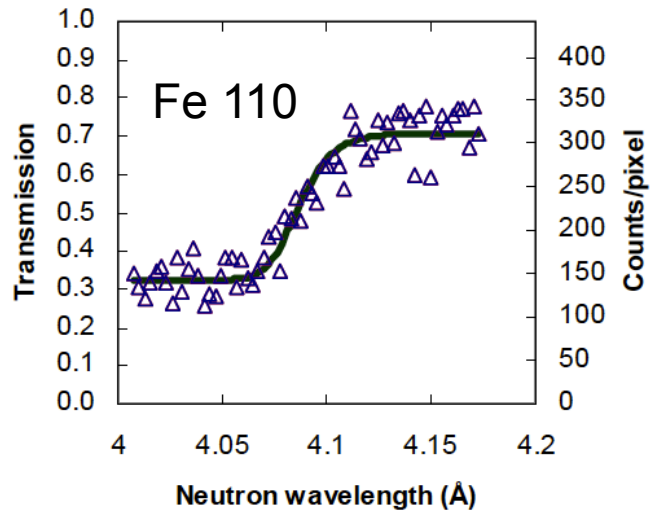
Courtesy of Prof. D. Penumadu, UTK and N. Kardjilov, HZB

Bragg Edge Imaging

- Strain mapping of steel screw



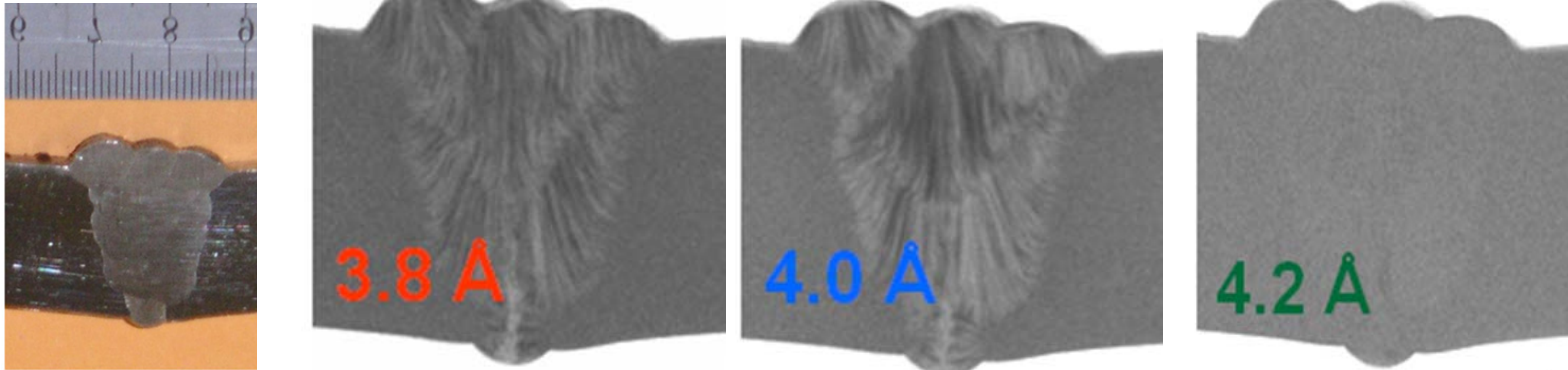
5 min exposure, 1 μs time res.



Strain map image of the steel screw. Strain values in μstrain

Bragg Edge Imaging

- Texture mapping



Bragg reflected neutrons result in narrow dips in the actual transmission at precise wavelengths specified by Bragg's law:

$$\lambda_{hkl} = 2d_{hkl} \sin\theta_{hkl}$$

where d_{hkl} is the interplanar distance for the (hkl) planes and θ_{hkl} are the Bragg angles θ_{hkl} depends on the relative orientation of the crystal lattice to the neutron beam.

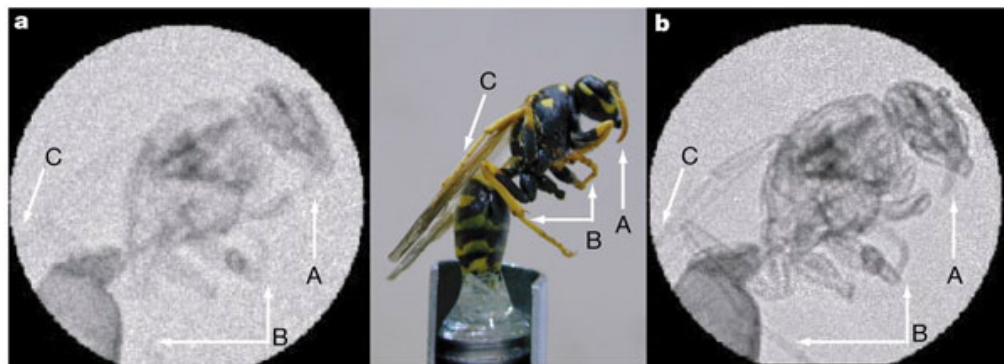
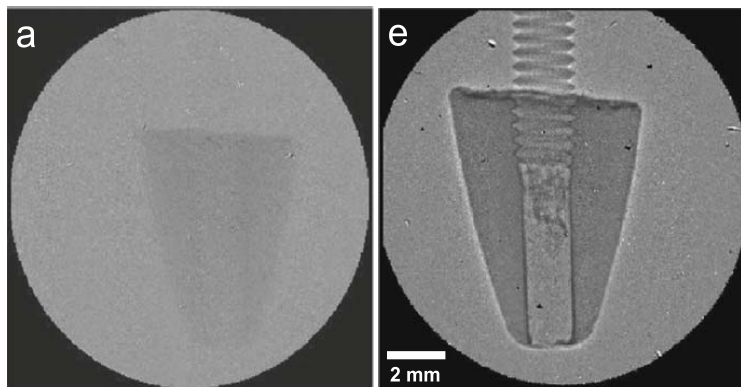
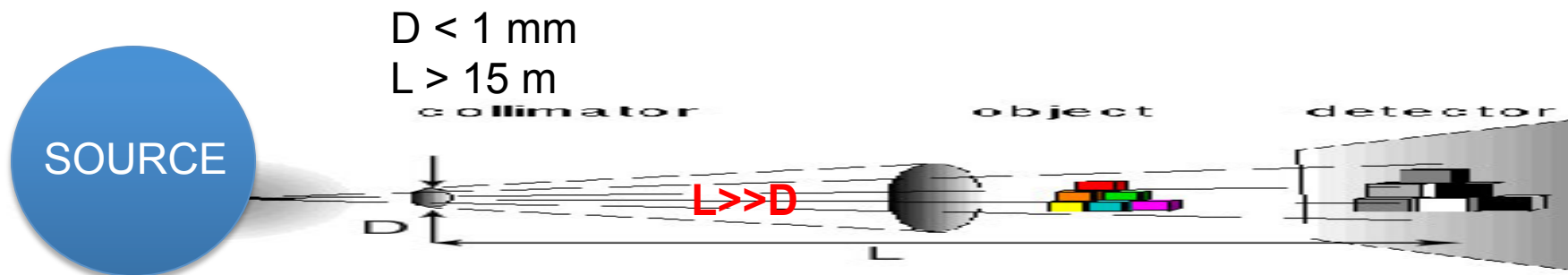
At λ_{hkl} , creation of map of the number of crystals having any of their (hkl) directions making an angle, β_{hkl} , with the incident beam given by:

$$\beta_{hkl} = (\pi/2) - \arcsin(\lambda_{hkl} / 2d_{hkl})$$

Kockelmann et al., NIM A, Vol. 578 (2007) 421.

Propagation-based Neutron Phase Imaging

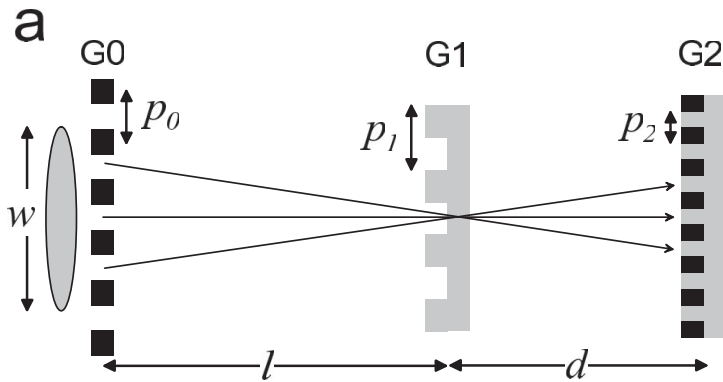
- Source needs to be spatially coherent (i.e. small pinhole and long pinhole-detector distances)
- Flux is low (up to 98% of flux is sacrificed, several hours to days for one radiograph)



(a) Neutron attenuation radiograph (e) and phase contrast radiograph of a lead sinker mounted on an Al screw. [B. Schillinger et al., *Mat. Trans. Proc.* (2006) 61]

(a) Neutron attenuation radiograph (b) photograph and (c) phase contrast radiograph of a yellow jacket wasp. [B. E. Allman et al., *Nature* 408 (2000) 158]

Phase Radiography using Grating Interferometry

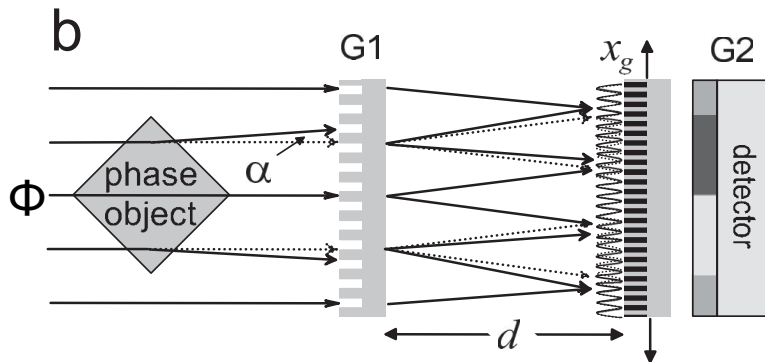


- G0 creates array of coherent sources from source w
- G1 creates diffraction patterns for each source which overlap if

$$p_0 = p_2 \frac{l}{d}$$

- Diffraction pattern has maximum contrast when d is a integer multiple of the Talbot length, L_T

$$L_T = \frac{p_1^2}{\lambda}$$



- Phase object cause distortion of diffraction pattern (or phase shift of incident wave Φ)
- Measure diffraction pattern by translating G2

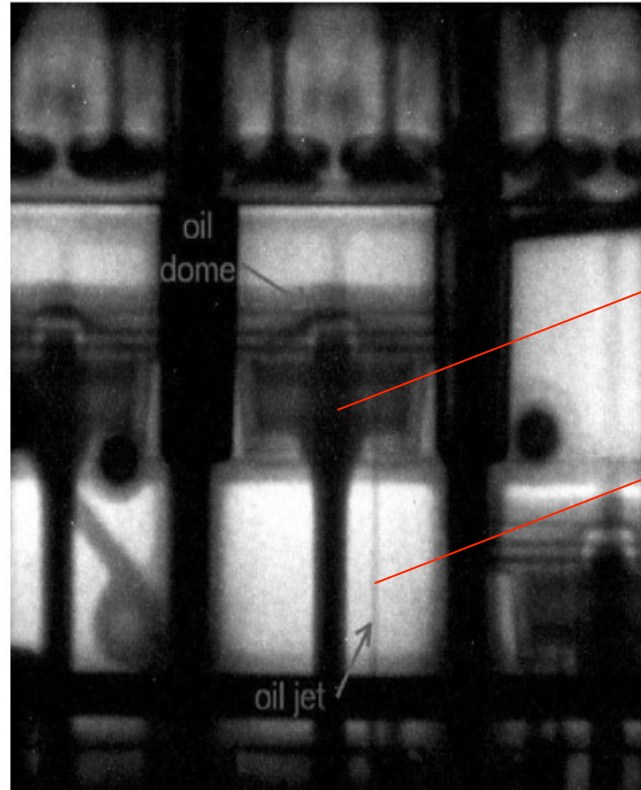
G0: (source) absorption grating, period p_0
 G1: phase grating, period p_1
 G2: (analyzer) absorption grating, period p_2

[Pfeiffer et al., **PRL**. 96 (2006) 215505]

$$p_0 \sim 1 \text{ mm}, p_1 \sim 10 \text{ } \mu\text{m}, p_2 \sim 5 \text{ } \mu\text{m}, l \sim 5 \text{ m}, d \sim 20 \text{ mm}$$

Stroboscopic imaging

- Makes a cyclically moving object appear to be slow moving
- Pulsed sources are by definition stroboscopic neutron sources



Oil spreading
into bottom of
piston

Oil jet
ejected into
bottom of
piston

Stroboscopic imaging:
150 exposures, 200 ms
each, 24 cm x 24 cm
field of view

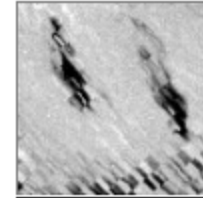
BMW engine, NEUTROGRAPH, ILL, France

Schillinger et al., NIM A **542** (2005) 142.

Applications at a glance

- Archeology
- Bio-medical
- Botany
- Contraband
- Cultural Heritage
- Energy
- Engineering/Materials Science
- Forensic Science
- Geology/Earth Sciences
- Homeland Security
- Paleontology
- Quality Assurance

Visualization of water transport in artificial soil sedimentation (20 s frame, 25 x 25 cm²)



<http://neutra.web.psi.ch/gallery/animations.html>

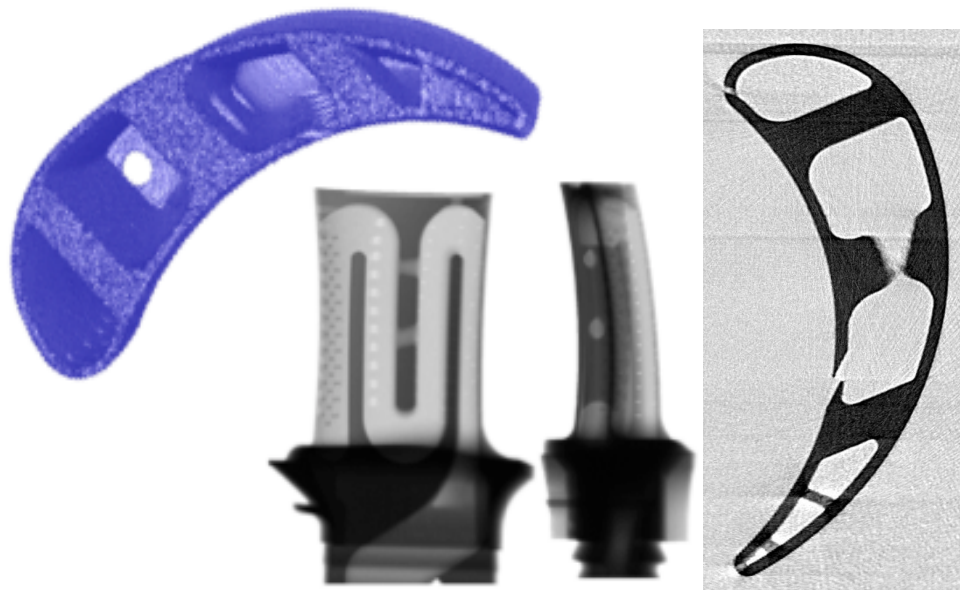
Radiography of a dry monkey skull



<http://neutra.web.psi.ch/gallery/biological.html>

Materials Research, Energy and Engineering Applications

Using neutron CT to study internal structure of turbine blades made by AM



ASM 100th ANNIVERSARY
1913-2013

am&p
ADVANCED MATERIALS & PROCESSES[®]

www.asminternational.org
MARCH 2013 • VOL 171, NO 3

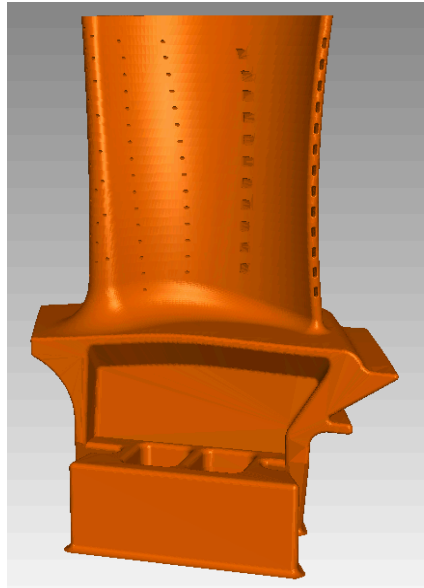
Materials for Aerospace

ICME & MGI •
Big Area Additive Manufacturing •
Neutron Characterization for AM •

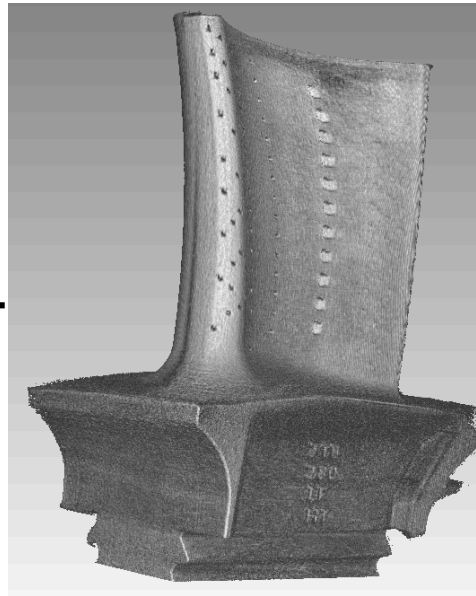
ASM
The Materials Information Society
Everything Material.
AN ASM INTERNATIONAL PUBLICATION

- New manufacturing techniques require advanced characterization capabilities for prediction and validation
- Neutron imaging data provide direct tests for model validation and process optimization

Fabrication tolerance studies using CAD drawing and neutron CT



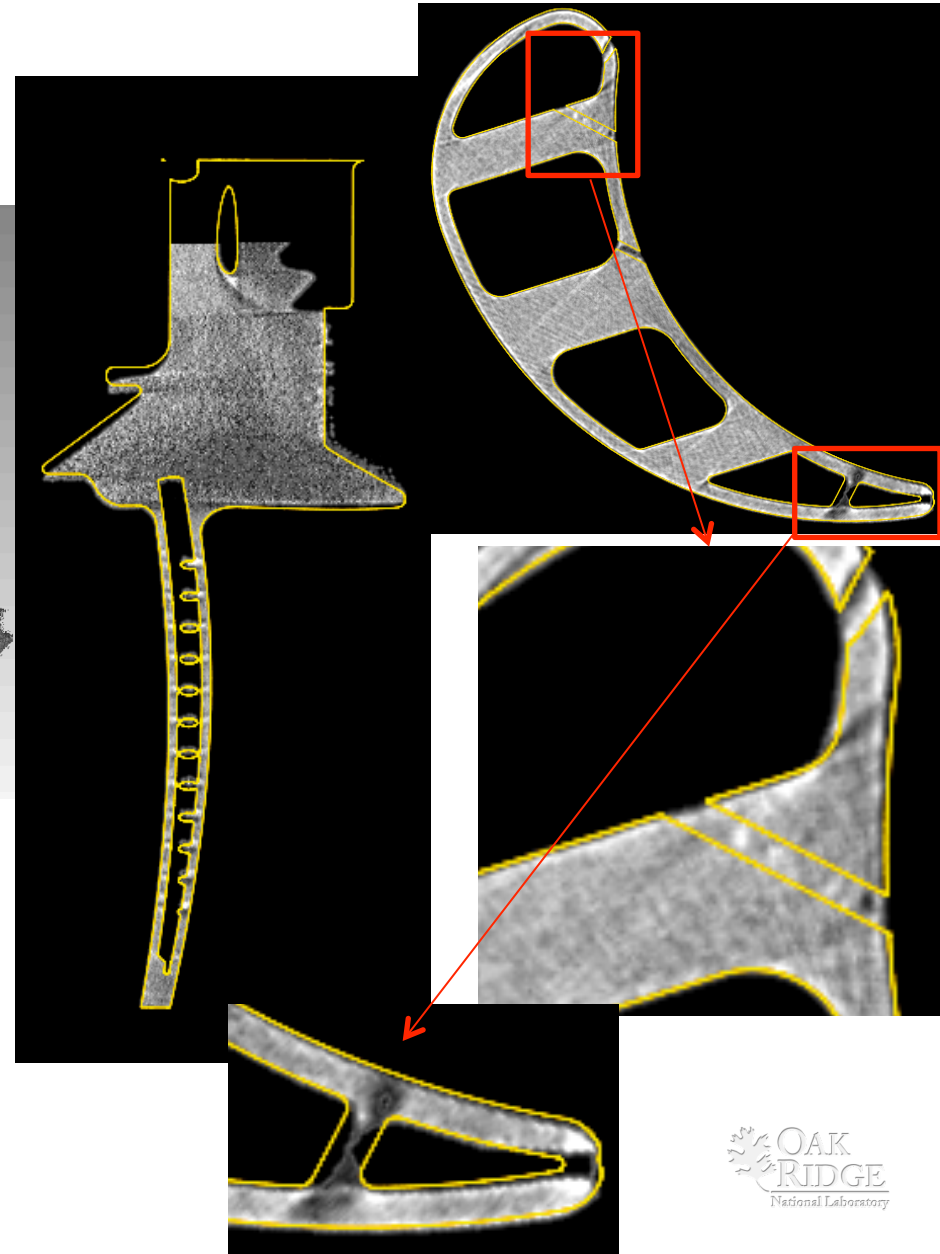
+



Engineering drawing

Neutron CT

- Semi-automated analysis
- 2 weeks of effort per sample
- Need for software capable of looking for features we don't know exist



Neutron Computed Tomography Characterizes Diesel Particulate Filter Regeneration Processes

Scientific Achievement

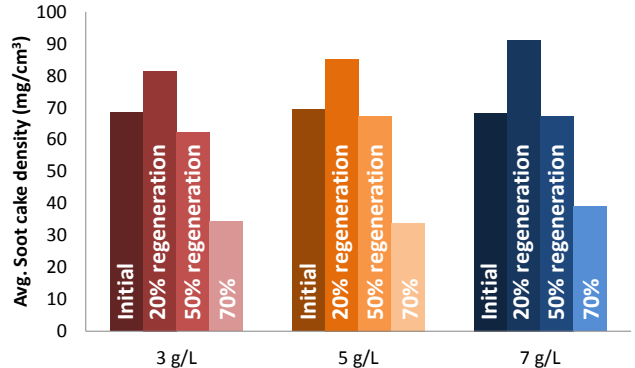
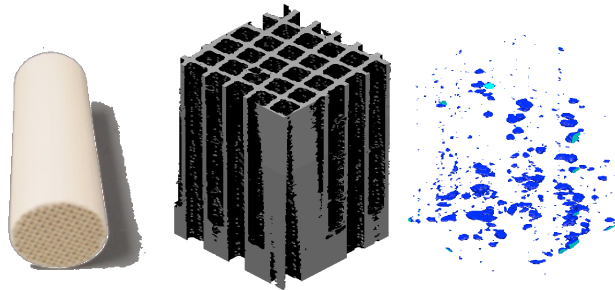
Soot cake properties and distribution in sequentially regenerated diesel particulate filters (DPF) were assessed quantitatively using Neutron Computed Tomography (nCT) maps

Significance and Impact

Measured soot cake properties enable industry modelers and engine controllers to improved predictions and achieve more fuel-efficient regeneration

Research Details

- Soot cake density, thickness and axial profile measured during sequential regeneration
- Different soot loading displayed same behavior during regeneration
- Highest soot cake density observed during initial 20% regeneration; afterwards porosity in the layer increases
- Quantitative findings directly relate to model parameters



(1) Photograph, neutron tomography results showing a virtual separation of DPF walls (2) and particulate matter. (3) Soot cake density measured during sequential regeneration

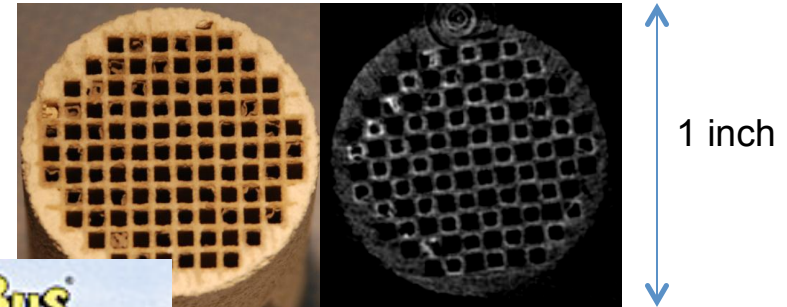
Nuclear Instruments and Methods in Physics Research A, 729 (2013) 581–588



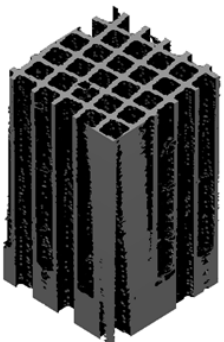
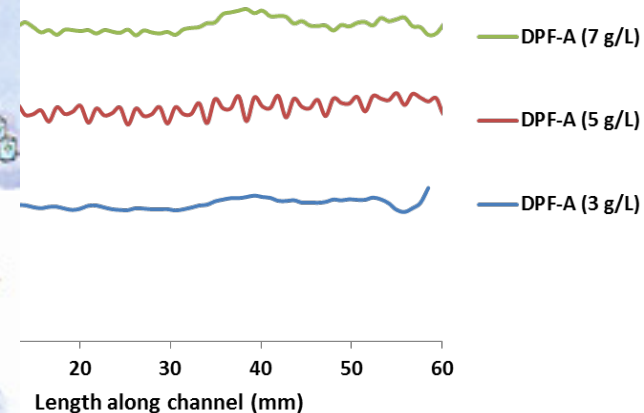
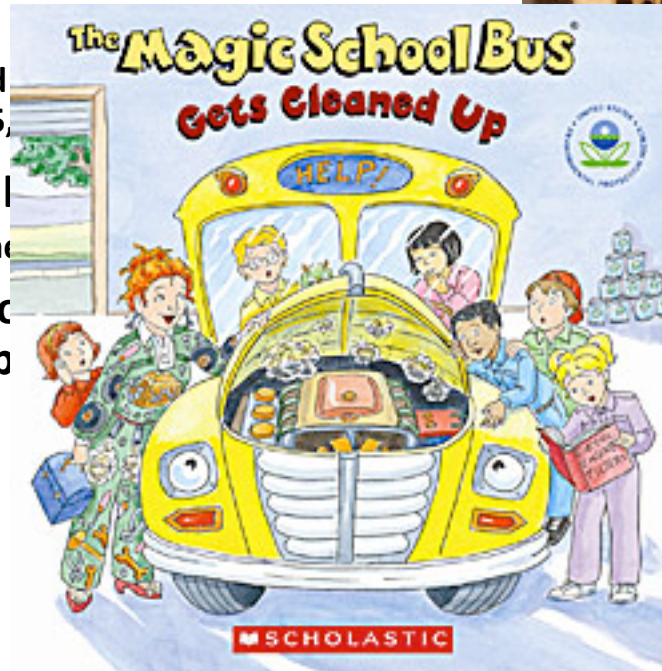
Non-destructive neutron imaging being employed to investigate automotive devices and functionality

- Unique and powerful neutron capabilities available at ORNL
- Neutron imaging is a non-destructive technique and analytical tool

Cross-sectional photograph (left) and equivalent neutron radiograph (right)



- Particulate distributions
 - Quantification possible
 - Average distribution and particulate loadings (3, 5, 7 g/L)
- Intra-fuel injector flow
 - More sensitive to fuel than neutron imaging
- Sophisticated image processing allows device tomography

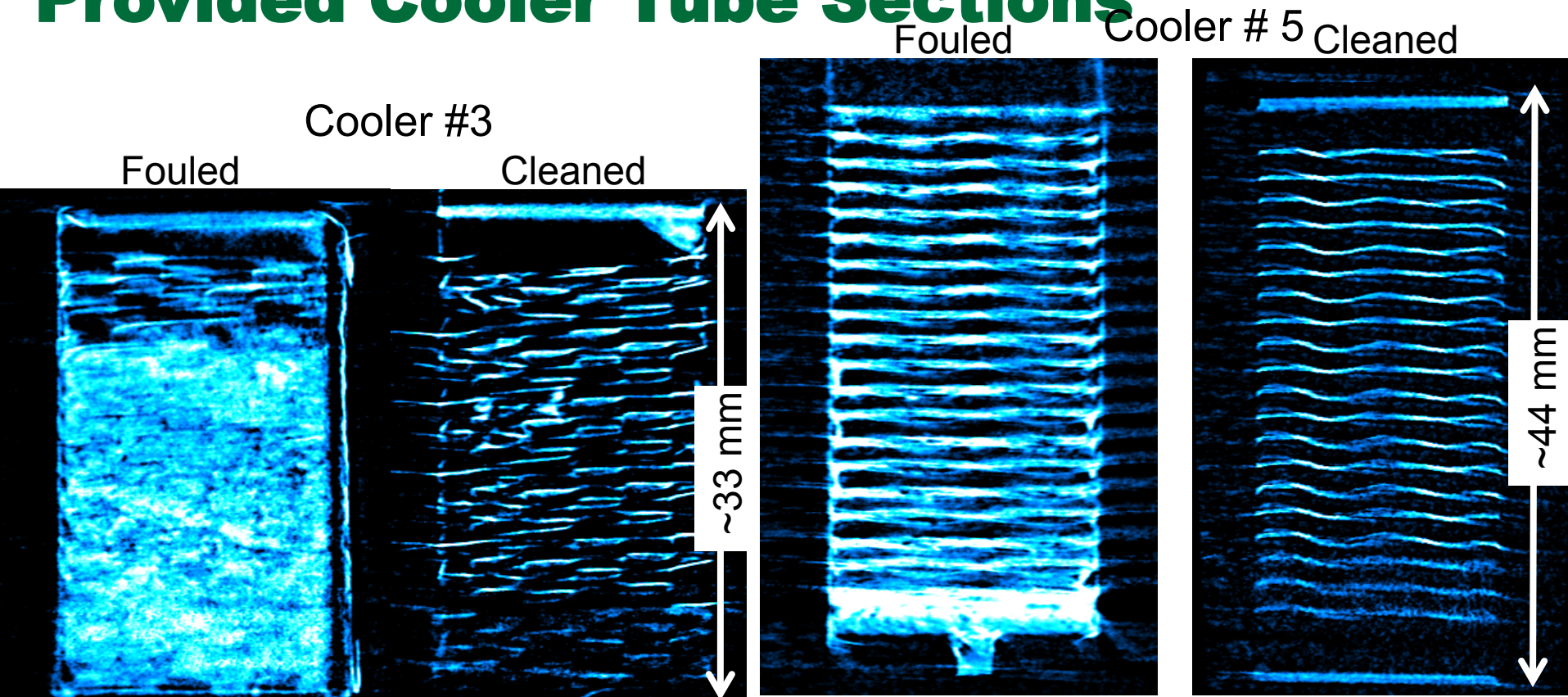


DPF Walls



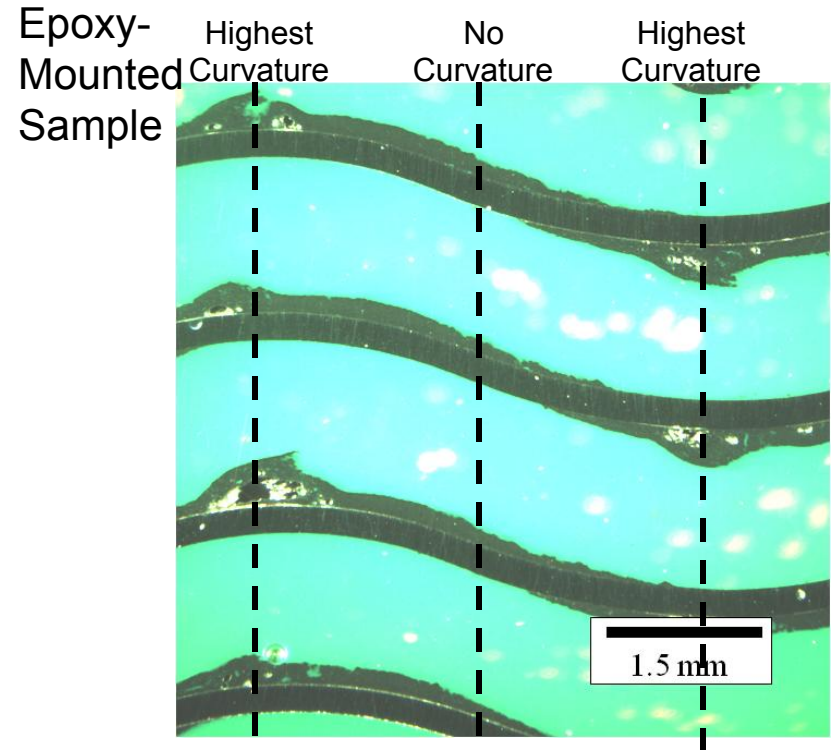
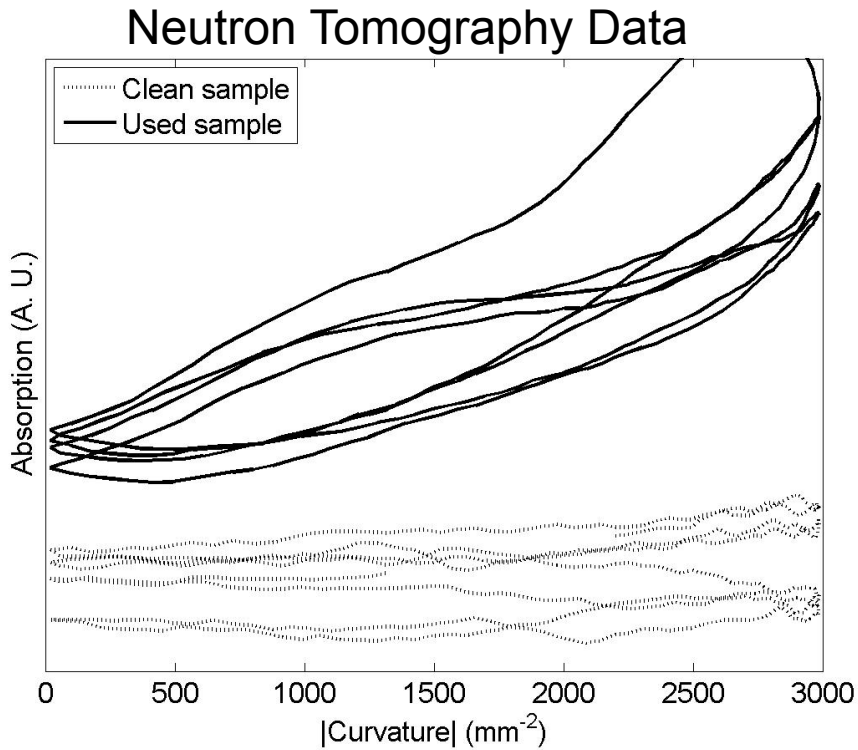
Particulate

Neutron Tomography of Industry-Provided Cooler Tube Sections



- Slices can be collected along any plane through the cooler.
- The resolution was not high enough to measure thickness directly but we can still gather useful information about the deposit location relative to the heat exchanger geometry.

Effect of Fin Curvature on Neutron Attenuation

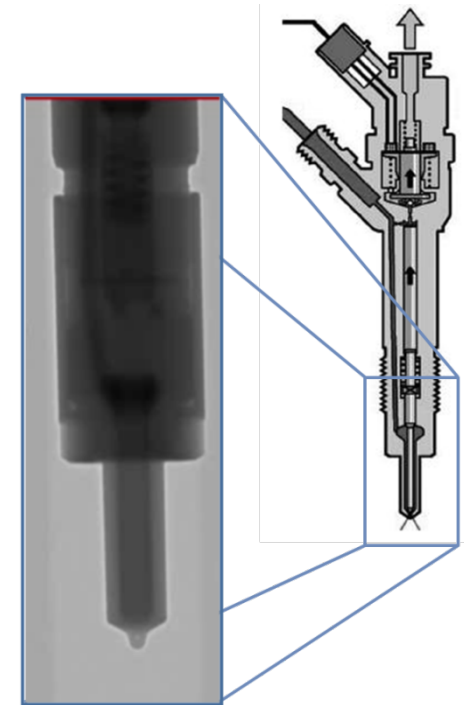


- Absorption is lowest at the inflection point of the sine wave and highest at the peaks/valleys which compares well to deposit location observed in the epoxy-mounted sample.

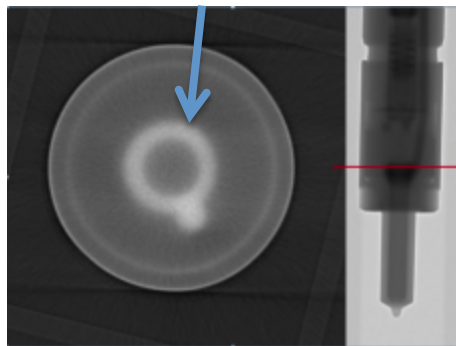
Filling Voids in Engine Research using Neutron Imaging

Diesel fuel injector study initiated to study intra-injector flow and near nozzle spray dynamics

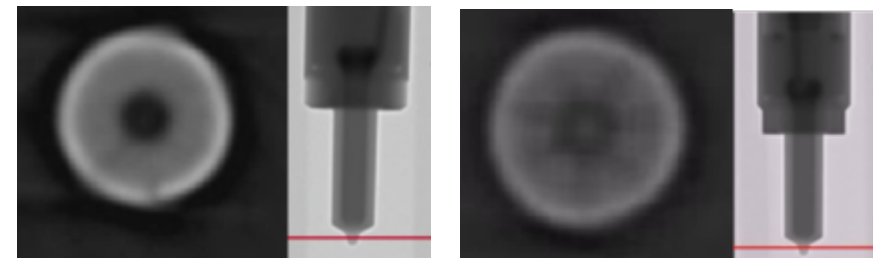
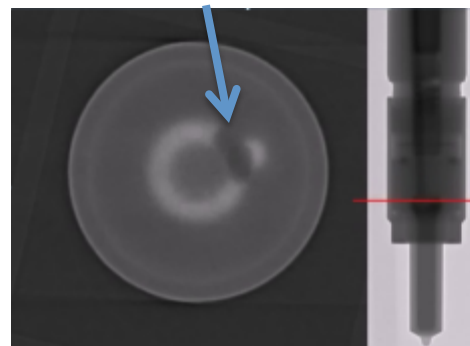
- Neutron imaging approach being employed to study fluid dynamics in diesel fuel injectors
- Able to see fluid void inside injector
 - Voids will be focus of efforts investigating cavitation
 - Cavitation is a major contributor to injector failure
 - Understanding under what conditions cavitation occurs is important as new, high-efficient combustion strategies are investigated
 - Broad impact as these in-cylinder injectors will start to become prevalent in gasoline vehicles (gasoline direct injection)
- Recently efforts have moved to dynamic spraying and imaging of both intra-injector flow and near nozzle spray dynamics.



Filled reservoir



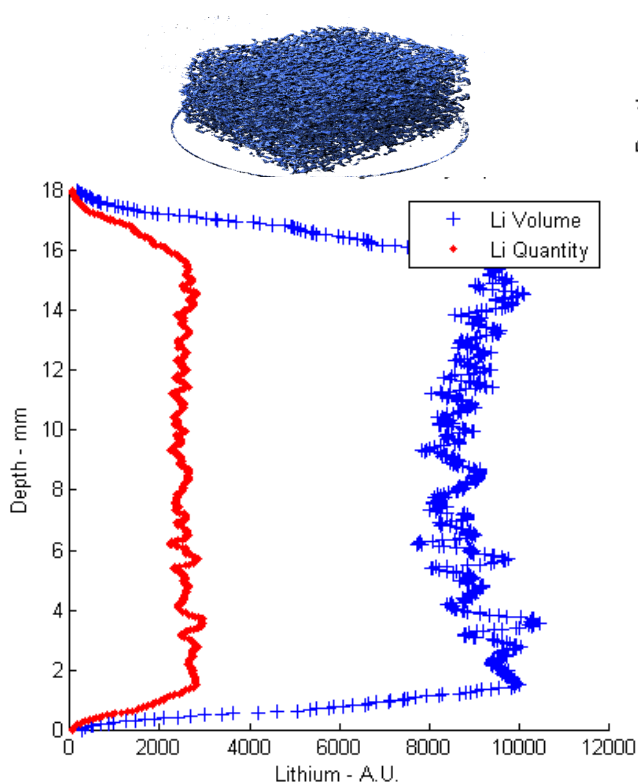
Void in reservoir



150 micron Pinholes visible in empty nozzles

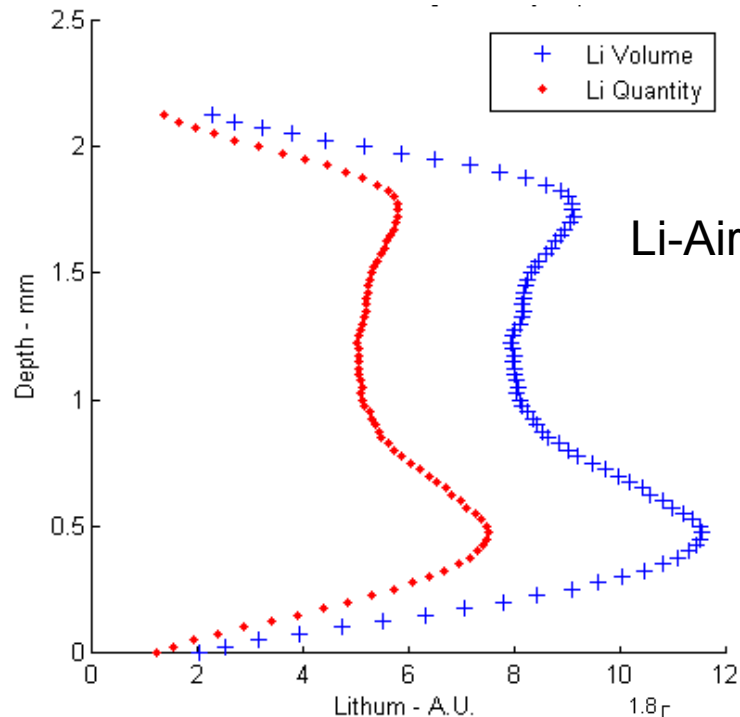
Higher contrast expected with fluid

Comparison of Li Distribution as a function of depth of battery

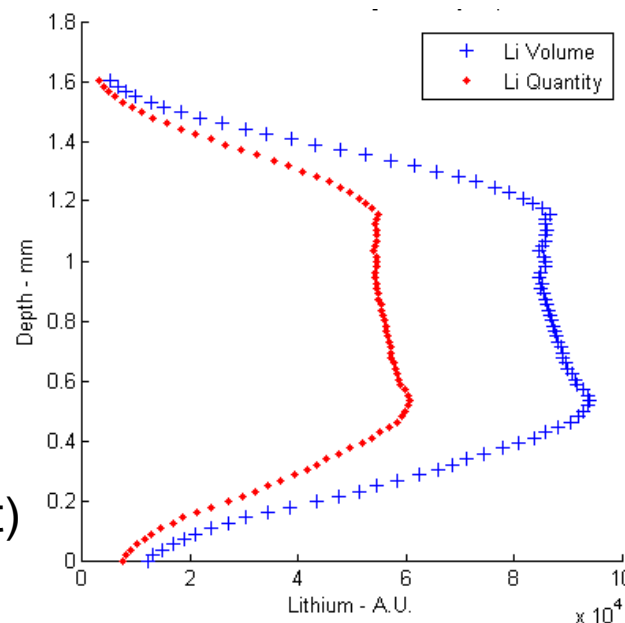
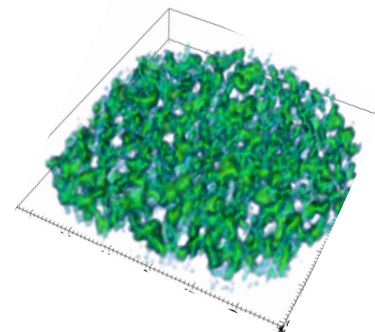


Control

Nanda et al., Journal of Physical Chemistry C, 2012.



Li-Air (no catalyst)

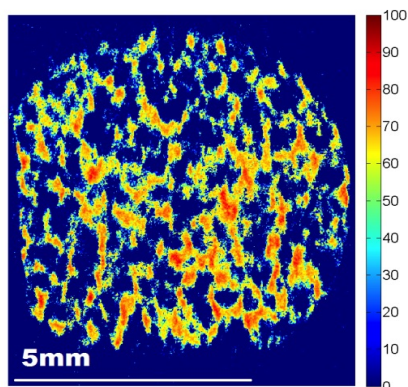


Li-Air (with catalyst)

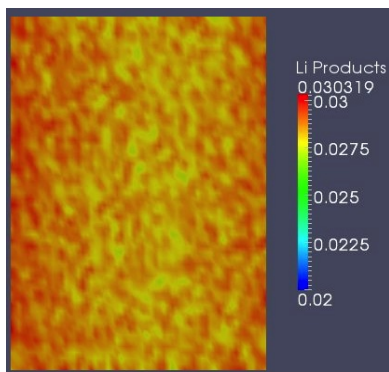
Neutron Imaging Provides the Basis for Developing Models

Non-uniform lithium distribution may limit rechargeability

Neutron image
Li- air cathode



3D model
Li-air cathode



- Reaction phase 3 dimensional modeling was used to predict results and compare with measurements
- Spatiotemporal reaction phase three-dimensional modeling of the electrodes also predicted a non-uniform lithium product distribution, confirming the neutron imaging result.
- Need to match resolution of neutron imaging capabilities to further improve feedback to modeling tools

THE JOURNAL OF
PHYSICAL CHEMISTRY C

Article

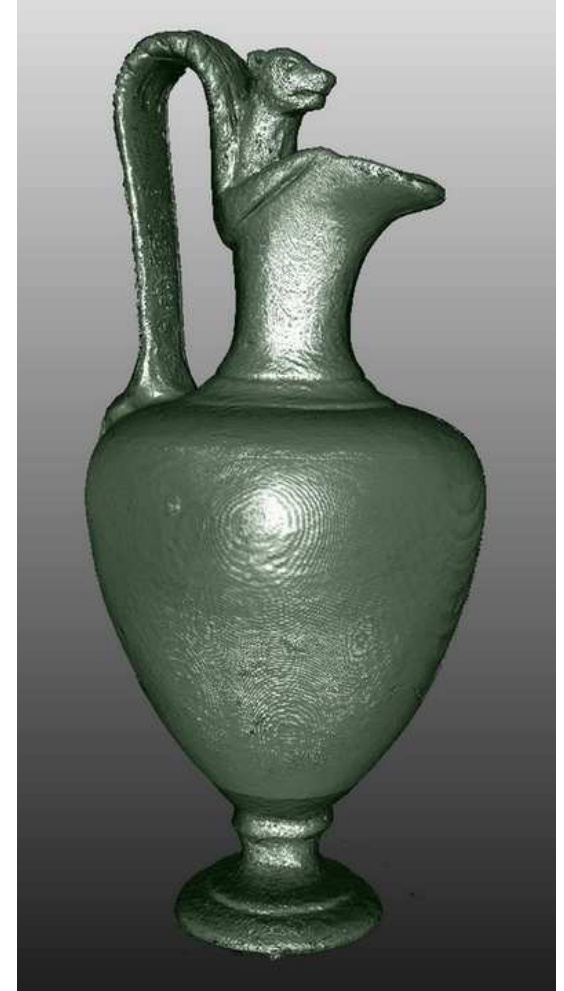
pubs.acs.org/JPC

Anomalous Discharge Product Distribution in Lithium-Air Cathodes

Jagjit Nanda,^{*,†} Hassina Bilheux,^{*,‡} Sophie Voisin,[‡] Gabriel M. Veith,[†] Richard Archibald,[§]
Lakeisha Walker,[‡] Srikanth Allu,[§] Nancy J. Dudney,[†] and Sreekanth Pannala^{*,§}

[†]Materials Science and Technology Division, [‡]Neutron Scattering Science Division, and [§]Computer Science and Mathematics Division, Oak Ridge National Laboratory, Oak Ridge, Tennessee 37831, United States

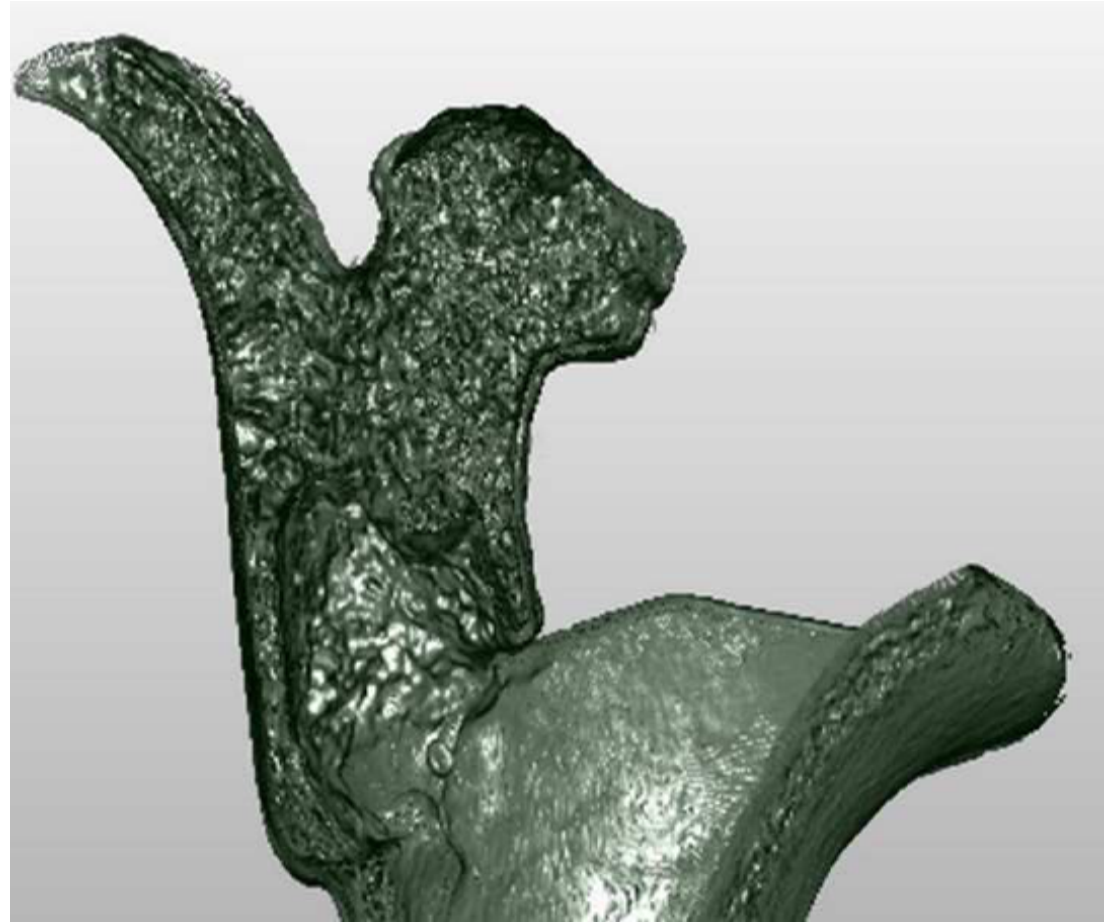
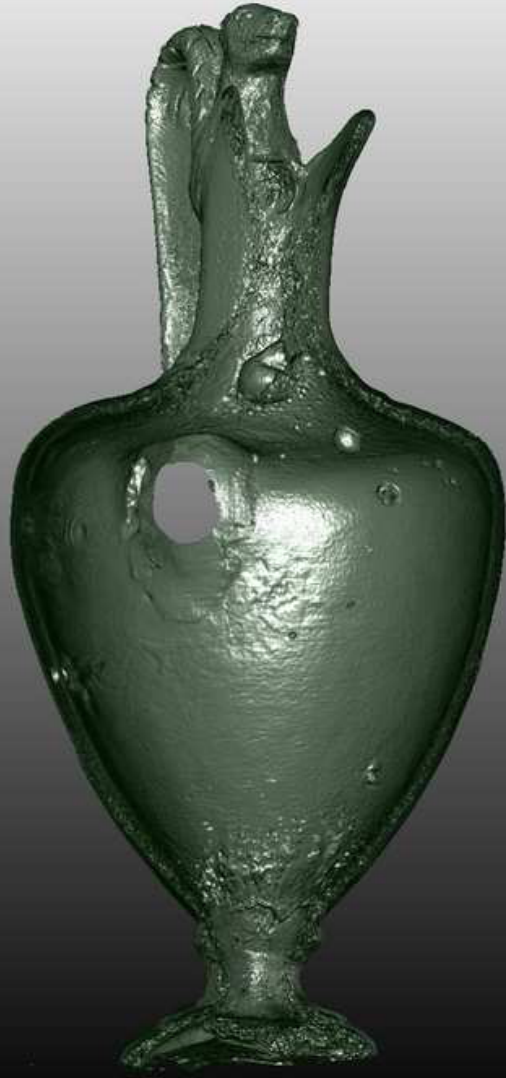
Ancient Craft Skills meet Modern Characterization



K. Ryzewski (PI), S. Herringer, H. Z. Bilheux, J.-C. Bilheux, B. Sheldon

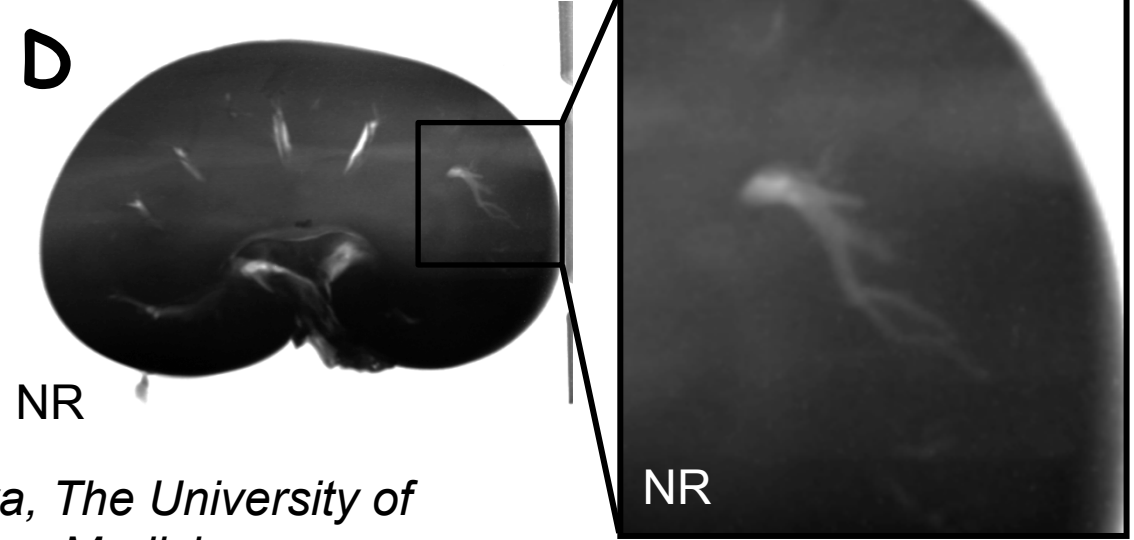
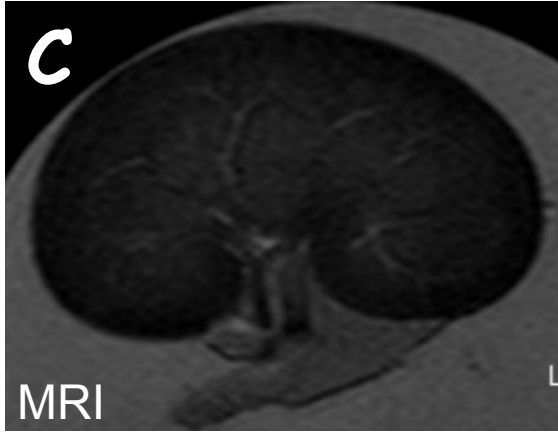
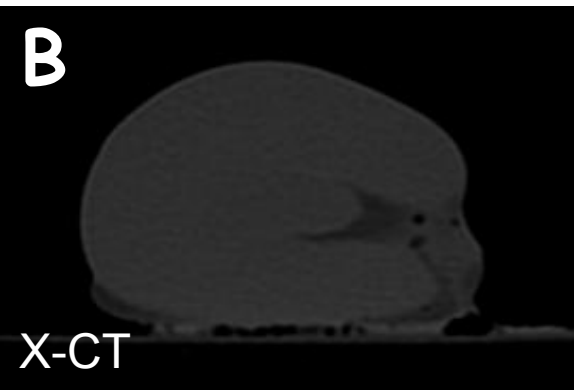
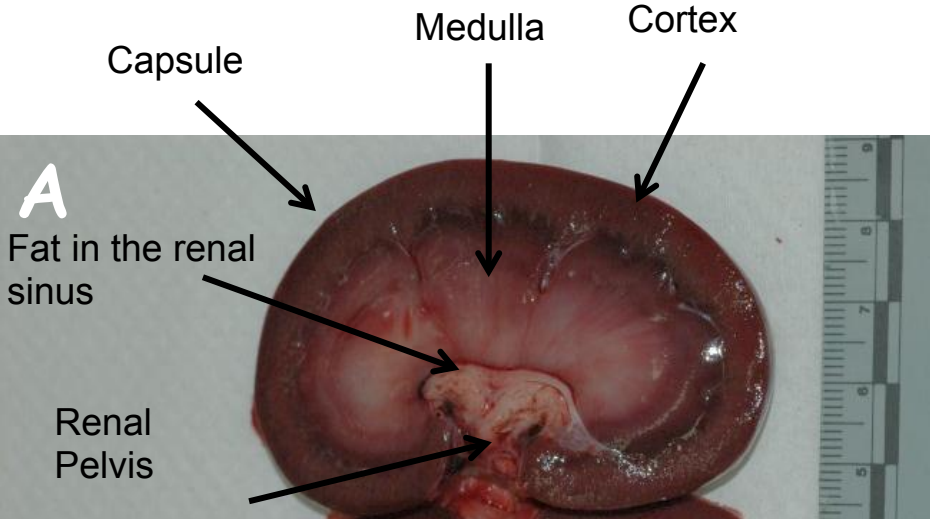
45 Managed by UT-Battelle
for the U.S. Department of Energy

Ancient Craft Skills meet Modern Characterization



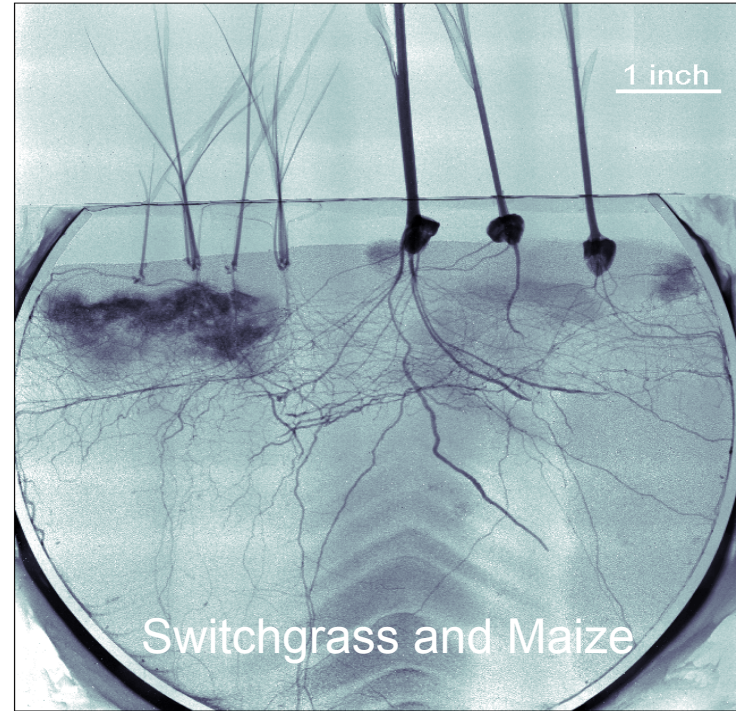
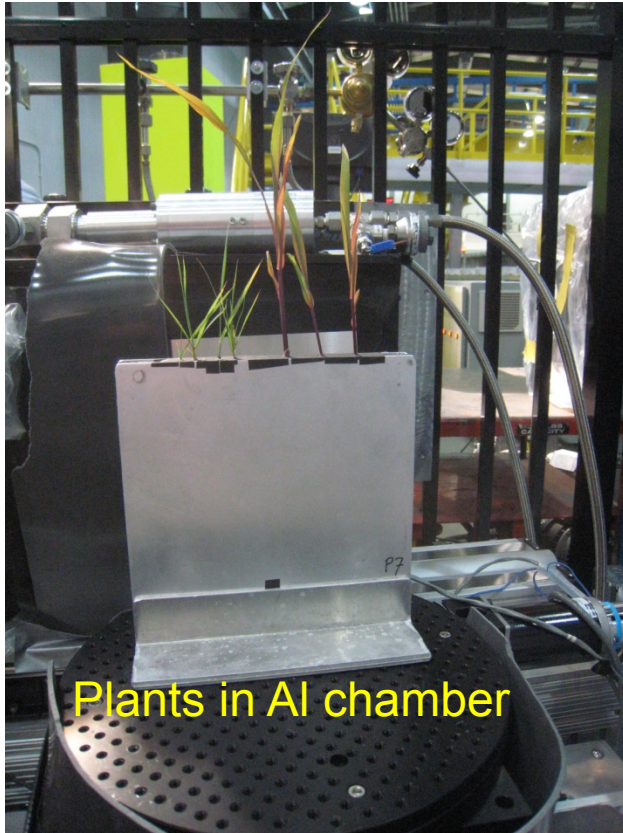
Biological and Environmental Applications

MRI, X-CT, and NR imaging techniques



Courtesy of Dr. Maria Cekanova, The University of Tennessee, College of Veterinary Medicine

Neutron Radiography of Roots at CG1-D



- Water injected into root zone at base
- Unidentified endophyte (symbiotic) or decomposer fungi visible near roots of switchgrass (left), revealing substantial hydration of the rhizosphere
- Both fine and coarse roots are readily visible

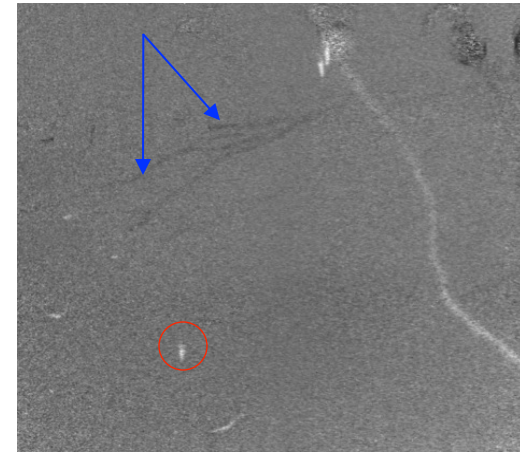
Changes in Soil and Root Water Content using Neutron Radiography



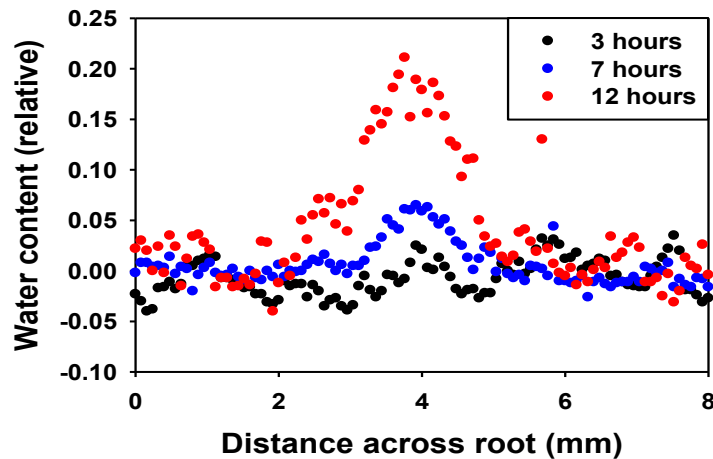
t = 0 h



t = 12 h



t = 12/t = 0

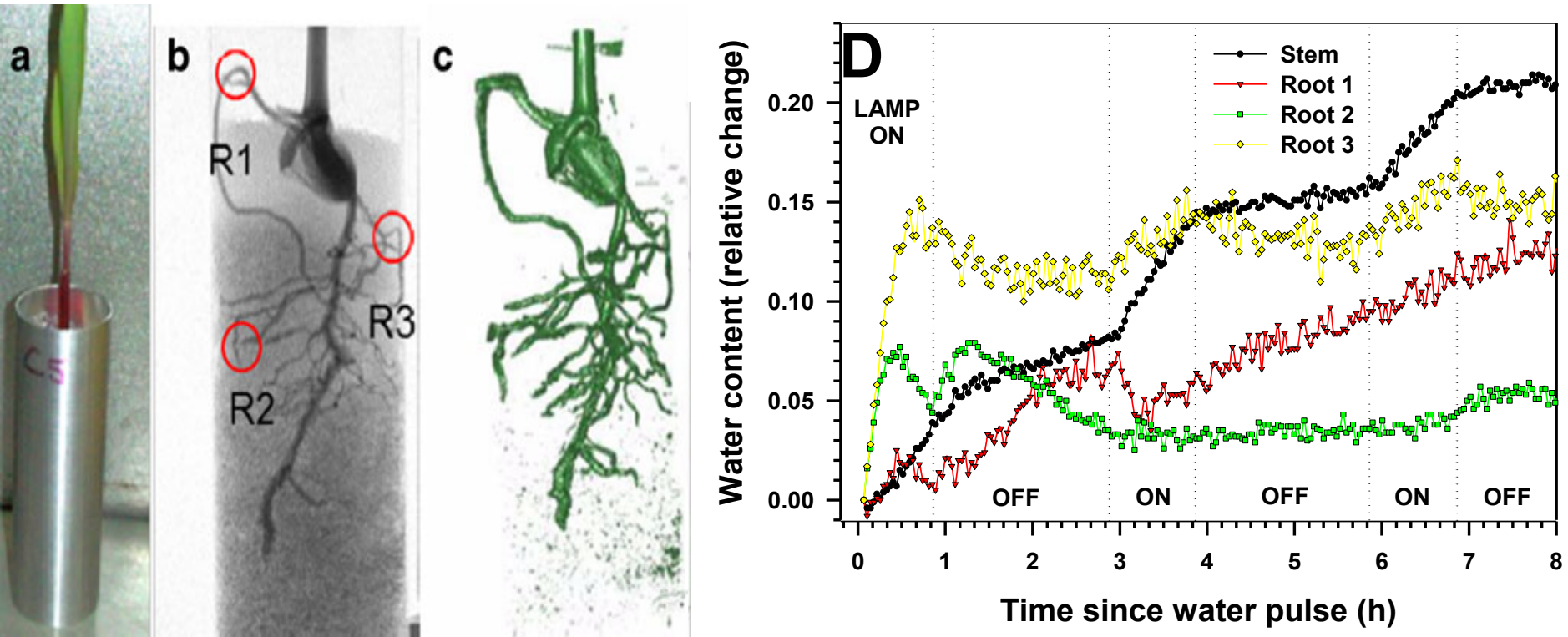


Top – More water showing up based on division (white areas)

Blue arrows show where water was removed from the system.

Left – increase in water content or root or rhizosphere due to root growth or root water efflux

Neutron sensitivity to H atoms and thus observe Water Uptake by Roots and Stem



10-d old maize seedling (A) aluminum sample chamber; (B) neutron radiograph at $\sim 70 \mu\text{m}$ pixel resolution illustrating roots distribution (0.2-1.6 mm); (C) 3D tomographic reconstruction; (D) Timing of water uptake by plant components highlighted in (B) illustrating impact of solar radiation on rate of water flux in stem and $\sim 0.5 \text{ mm}$ first and second order roots.

➤ This study provides direct evidence for root-mediated hydraulic redistribution of soil water to rehydrate drier roots

Thank you

(bilheuxhn@ornl.gov)

Courtesy of
Prof. Krysta Ryzewski, Wayne
University
Susan Herringer, Prof. Brian Sheldon,
Brown University

